

Master Thesis
Sports Technology
10th semester



Authors: Lasse Jakobsen & Frederik Husted Ahlers

Group number: 16gr10200

Supervisors: Mark de Zee & Christian Gammelgaard Olesen



TITELINDBERETNING

Bachelorprojektets/specialeprojektets titel kommer til at stå på dit bevis, og du bør derfor udfylde blanketten meget omhyggeligt.

Bemærk, at der som minimum kræves en engelsk titel, før dit bevis kan udstedes.

Blanketten afleveres sammen med bachelorprojektet/kandidatspecialet til din studiestekretær.

Dansk titel (Bachelorprojektet/specialeprojektets titel (max 4 x 60 karakterer))

Engelsk titel (Bachelorprojektet/specialeprojektets titel (max 4 x 60 karakterer))

Biomechanical analysis of hand cycling propulsion movement: A musculoskeletal modelling approach
&
Development of a wireless crank moment measurement-system for a handbike: Initial results of propulsion kinetics

Forfattere			Uddannelse	
			Bachelor/ Diplomingeniør	Kandidat
	Navn	Cpr-nr eller studienr		
1.	Frederik Husted Ahlers	20113004	<input type="checkbox"/>	<input checked="" type="checkbox"/>
2.	Lasse Jakobsen	20113044	<input type="checkbox"/>	<input checked="" type="checkbox"/>
3.			<input type="checkbox"/>	<input type="checkbox"/>
4.			<input type="checkbox"/>	<input type="checkbox"/>
5.			<input type="checkbox"/>	<input type="checkbox"/>
6.			<input type="checkbox"/>	<input type="checkbox"/>
7.			<input type="checkbox"/>	<input type="checkbox"/>
8.			<input type="checkbox"/>	<input type="checkbox"/>

Udfyldes af studiestekretæren:

Dato: _____ Underskrift: _____

Blanketten sendes til Det Sundhedsvidenskabelige og Det Teknisk-Naturvidenskabelige Fakultetskontor, Eksamenskontoret, Niels Jernes Vej 10, 9220 Aalborg Øst



Development of a wireless crank moment measurement-system for a handbike: Initial results of propulsion kinetics

Lasse Jakobsen¹ & Frederik Husted Ahlers²

Abstract

Objective: Develop a wireless crank moment measurement system for a handbike. **Method:** A tee-rosette strain gage was mounted on the crankshaft and connected to a wireless transmitter. An optical wheel encoder provided crank position and speed data in order to determine applied crank force with respect to position and calculation of power. **Results:** Linearity ($R^2=1$) was demonstrated between applied force and voltage output for 1,2,3,4 and 5 kg load for the calibration procedure. The initial propulsion measurement presented data for applied crank moment, tangential force, angular velocity and power with respect to crank position. **Discussion:** This system can provide kinetic data in terms of tangential external force, provided by the athlete and as input for biomechanical modelling. This system has the potential to obtain field measurement on the road, due to the wireless system.

Keywords: Handbike, hand cycling, propulsion force, strain gage

Introduction:

Pedal force measurements are common in the scientific research field of cycling. The information of the force magnitude and direction on the pedals can be analyzed and force production effectiveness can be identified. (Bini & Carpes 2014). This would also be applicable for optimizing hand cycling propulsion effectiveness, though it is rarely seen (Arnet 2012b). For people with lower limb impairments, hand cycling as a sport activity has become popular since it was implemented in the Paralympic Games in 2004 (Faupin & Gorce 2008). Thus, the interest in relation to performance optimization has likewise arisen in the field of hand cycling, where the handbike interface has been under investigation (Arnet 2012b, Faupin & Gorce 2008, Goosey-Tolfrey, et al. 2008, Litzenberger et al. 2015). Depending on the specific research scope, propulsion force measurements can be used for analysis of performance. Additionally, propulsion force measurement can provide input for biomechanical models. A wide range of commercially available power sensors already exist on the market such as the SRM power meter, Quarq power meter and Garmin Vector power meter (Garmin, SRM, Quarq). Common for all systems is an average measure of power output for a number of complete revolutions. Hence, these systems do not provide detailed force information for a single propulsion cycle. Detailed force measurements in the scientific research field of hand cycling, is however determined in various ways and varies in accuracy and detail as well (Arnet 2012b, Bafghi et al. 2008, Verellen et al. 2004). The system developed by Arnet (2012a) implied an FS6-500 force sensor (AMTI,

¹ lasse@stagsted.net - M.Sc Stud. Aalborg University

² frehust@gmail.com - M.Sc Stud. Aalborg University



Crowthorne, England), measuring forces in three directions and therefore provided a detailed force measurement. With this system, Arnet (2012a) found that the tangential force during the hand cycling propulsion was the most dominant (Arnet 2012a). However, the FS6-500 is an expensive and wire based sensor, thus a large and heavy wire must follow the handbike handle during the propulsion and are unsuitable for force measuring on the road. This leads to the aim of this technical note, which was to provide technical information on a wireless and relatively inexpensive crank moment measurement system and to document its accuracy.

Method and materials

The procedure of this technical note consisted of two main steps.

1. Develop a system able to measure moment applied to the crankshaft during hand cycling propulsion.
2. Collect initial propulsion measurement data for crank moment applied to the crankshaft over the propulsion cycle.

1. System design

The system must meet the following overall requirements:

- Force measurement of the tangential force applied to the crankshaft for each revolution, during hand cycling.
- Determination of crank position and angular velocity.
- Synchronize force and crank position data, in order to locate force with respect to crank position and calculate power.

The system design was subdivided into “force measurement”, “calibration”, “crank position measurement” and “force and position synchronization”, in order to acquire the three requirements stated above. For “force measurement”, “crank position measurement” and “force and position synchronization” a set of requirements for each subpart was determined, in order to ensure acceptable data quality.

Force measurement

The force measurement part of the system must meet the following requirements:

- Measure crankshaft moment and thereby tangential force applied to the pedals, during the hand cycling propulsion movement.
- Sample at least 20 HZ in order to detect the changes in force for one propulsion cycle. The minimum sampling rate is based on the force measurement characteristics when propelling a



handbike with 60-70 rpm, obtained by Arnet et al (2012a) and accounts for Nyquist minimal sampling rate.

- Sample wireless in order to avoid entangling wires, during hand cycling propulsion.

When force is applied to the pedal, the crankshaft is submitted to torsion. During torsion, the principal normal stresses occur at an angle of $\pm 45^\circ$ with respect to the longitudinal axis of the crankshaft (Hoffmann 1989a). Therefore, a CEA-XX-125UT-350 tee-rosette strain gage (Micro measurement, Wendell, USA) was mounted on the crankshaft surface between the two crank bearings at an angle of 45° , with respect to the longitudinal axis. The strain gage was mounted between the crank tooth wheel and the right handle. Thus, the measure for crank moment did only correspond to the force contribution from the right arm. The tee-rosette contains two strain gages oriented at 90° with respect to each other. The strain gage was setup as a Wheatstone half-bridge circuit (Hoffmann 1989b).

The tee-rosette strain gage was connected to a V-Link[®]-LXRS[®] Wireless 7 Channel analog input sensor node (LORD Corporation, Williston, USA), according to the node manual (LORD 2015). The node was mounted at the left crank arm, thus it rotated in sync with the strain gage during the propulsion cycle. Sample rate was set to 512 HZ with one sensor input channel enabled. The sensor analog data was digitized in the node and wirelessly transmitted to an WSDA[®]-Base-101 Analog Output Base Station (LORD, Corporation, Williston, USA), connected to a laptop running node commander 2.17.0 (LORD Corporation, Williston, USA). Simultaneously, the analog output from the base station was wire-connected to a NI USB-6008/6009DAQ USB Device (National Instruments, Texas, USA) as illustrated in figure 3.

Calibration

In order to determine the crank moment from the voltage output given from the strain gage, a calibration procedure was performed. Thus, a specific voltage output corresponded to a specific applied crank moment.

The crank was locked vertically in a vice, as close to the crank box as possible. The pedal arms were placed horizontal at 90° with respect to vertical and the crank tooth wheel was fixed in this position. A string was fastened on the right pedal arm and loaded with 1,2,3,4 and 5 kilograms respectively. For every load, the voltage output from the strain gage changed and was sampled for five seconds. The average of the five second samples represented a measuring point for each load condition.

The setup is illustrated in figure 1. The procedure was repeated three times with three different gains ± 1 mV(gain 1214), ± 2.5 mV (569) and ± 5 mV(gain 291).

The calibration wizard in node commander was performed for all gains prior to applying loads (LORD 2015).

Crank position measurement

The part of the system determining the crank position must meet the following requirements:

- Determine crank position and angular velocity for each crank revolution.
- Be low frictional in order to minimize braking effect.

The position measurement must determine crank position with respect to applied moment. In addition, the position measurement must provide velocity data for power calculation (Watt). In this context, a HEDS-5540-A06 optical wheel encoder (Hewlett Packard, California, USA), with 500 impulses per revolution was used as the device for crank position determination. A tooth wheel was mounted on the crankshaft and connected to a second tooth wheel, mounted on a shaft entering the encoder. Hence, one revolution for the crankshaft corresponded to one revolution for the encoder and therefore 500 impulses. The CAD model of the crank position system is illustrated in figure 2.

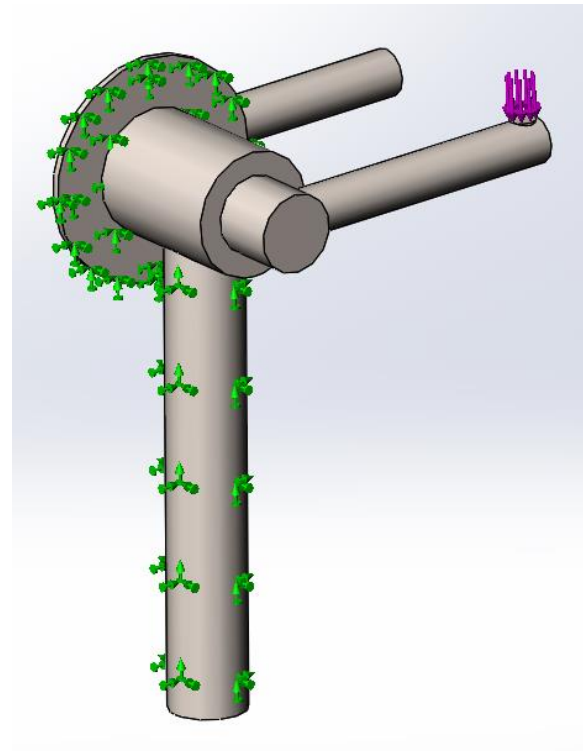


Figure 1: Calibration illustration (green arrows illustrates the fixed surfaces and the purple arrows represents applied force)

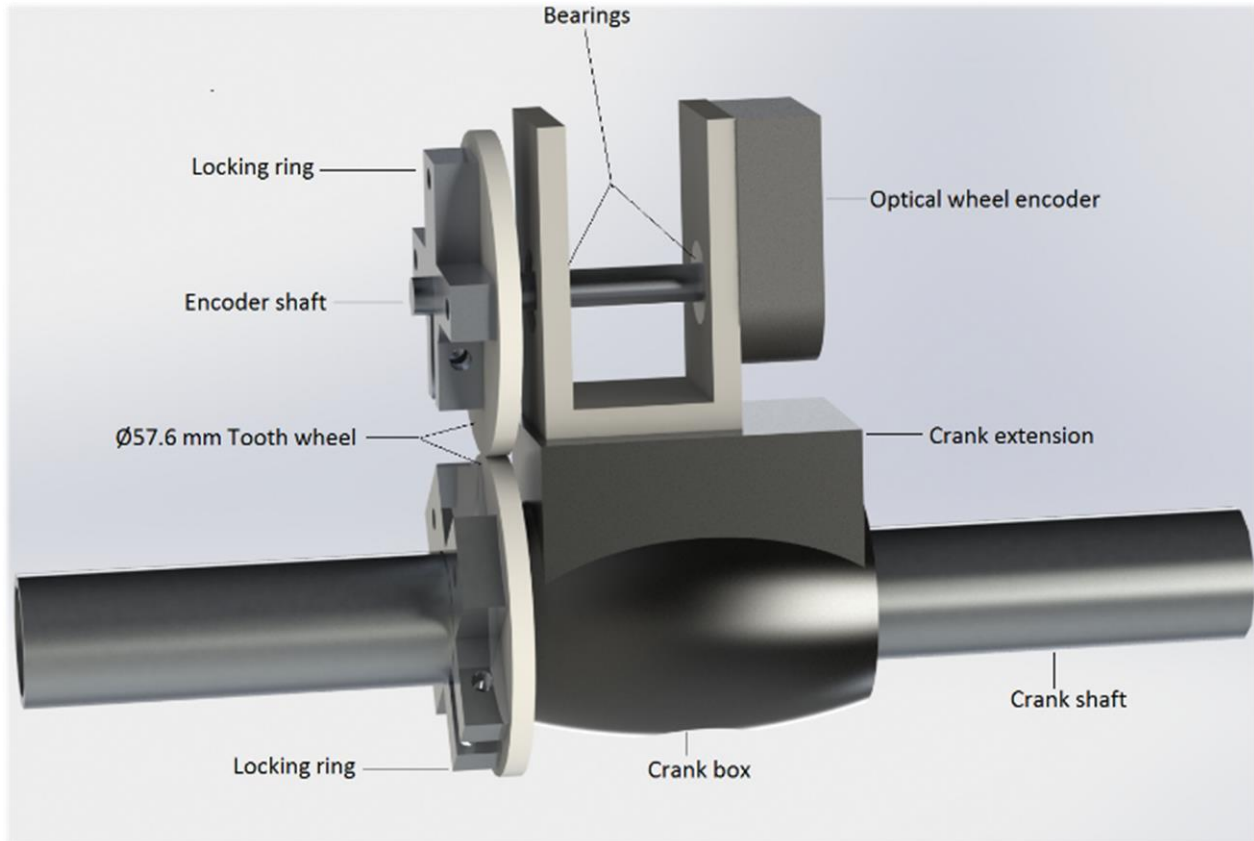


Figure 2: Crank position CAD model

The encoder contained an A channel and a 90° phase shifted B channel, enabling the ability to determine rotation direction. Like the WSDA[®]-Base-101 Analog Output Base Station, the encoder was also connected to the NI USB-6008/6009DAQ USB Device, where the analog encoder signal was digitized. The connection is presented in figure 3.

Force and position synchronizing

The force and position synchronizing subpart of the system must meet the following requirements:

- Sample at least same frequency as the wireless node connected to the strain gage, in order to avoid data loss.
- Position measurement and force measurement must be synchronized.

In order to determine the crank position with respect to the crank moment, the data were synchronized. As described previously, the force measurement and the position measurement subpart of the system, were connected to the NI USB-6008/6009DAQ USB Device. Thus, both signals were entering the same A/D converter simultaneously. A GUI (Graphical user interface) was set up in LabVIEW 2015 sp 1 (National Instruments, Texas, USA), with a live display for crank position and voltage given from the strain gage. The

tube. The backrest was placed in an angle of 158° with respect to horizontal (see figure 4). At the crank start position, the pedals pointed vertically towards the ground. Resistance was controlled with the Bluetooth Powered Cycling and Running Workout Tracker 5.7.7 application (Wahoo Fitness, Atlanta, USA) and set to 35%.

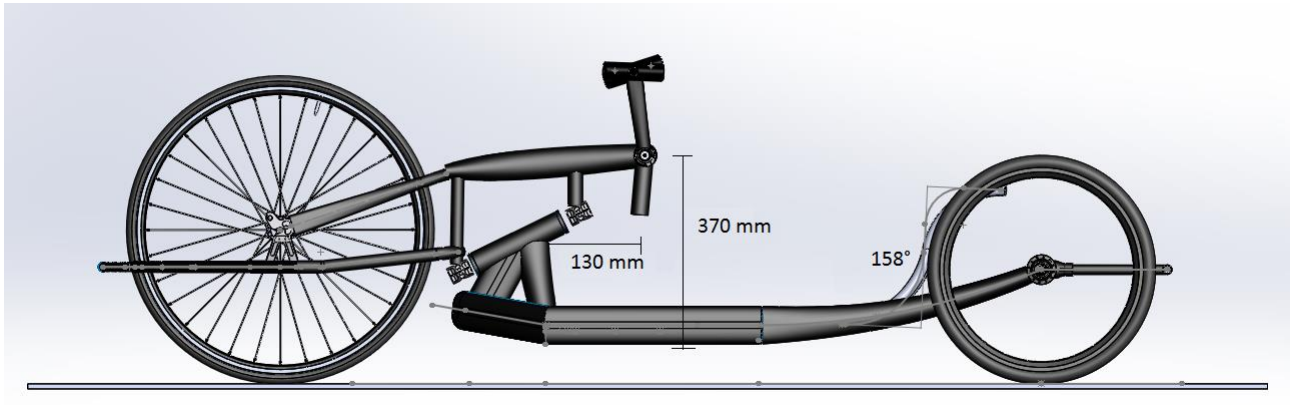


Figure 4 : Handbike setup. Measures of crank position (370 mm vertically to the base plate, 130 mm horizontal with respect to the vertical tube connected to the head tube and backrest angle of angle of 158°)

The subjects' anatomical location with respect to the crank is illustrated in figure 5, where it is evident that the shoulder and elbow joint is located below the crank.

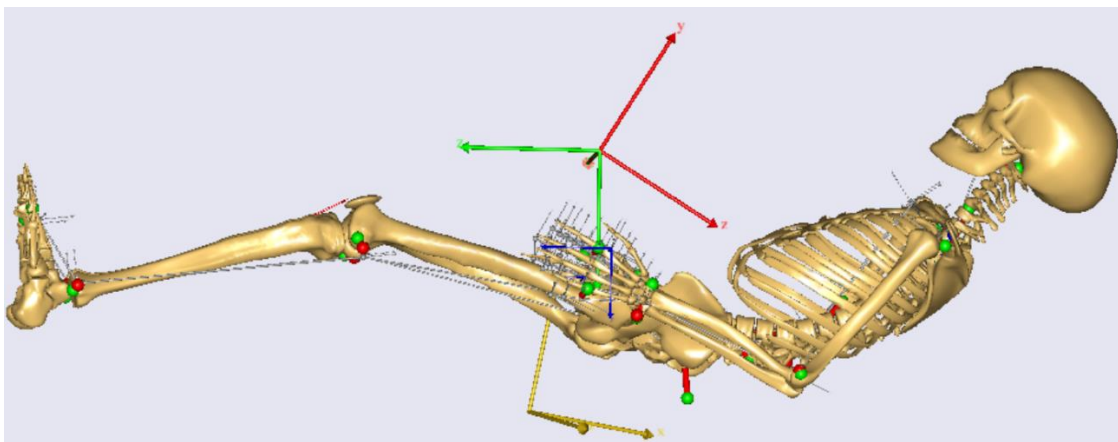


Figure 5 : The crankshaft is represented by the red and green coordinate system. The shoulder position is located below the crank and the power output, tangential force and crankshaft moment will reflect the position.

Data analysis

For the calibration, coefficient of determination (R^2) was calculated between voltage and applied force. The 500-encoder impulses, representing one crank cycle, were divided by 360° leading to 1.389 impulses per degree. The raw data for the initial propulsion measurement was filtered with a Butterworth 10 HZ low pass filter. Data processing was done in MatLab R2015b (MathWorks, Incorporation, Massachusetts, USA) and Excel 2013 (Microsoft, Washington, USA).



Results

Calibration: The results for the calibration procedure is illustrated in figure 6 and represent the correlation between the applied load and the voltage output for 1 mV, 2.5 mV and 5 mV gain. The correlation value R^2 was 1.0 for all three gains, thus representing a linear correlation.

Wireless delay test: The wireless delay test found a delay of 4 ms when converting and transmitting the signal from the V-Link®-LXRS® Wireless 7 Channel analog input sensor node to the WSDA® -Base-101 Analog Output Base Station.

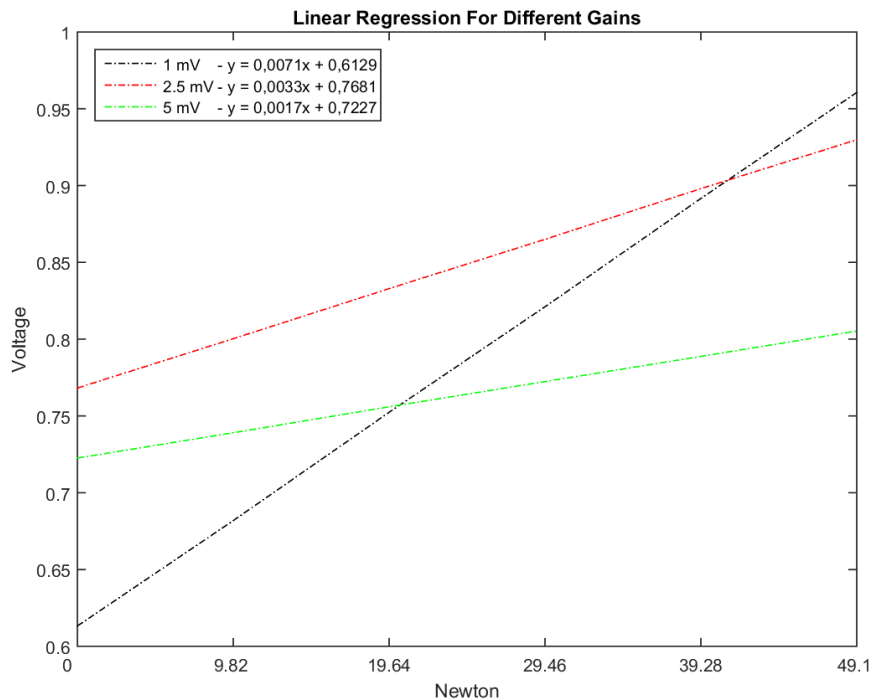


Figure 6 : Correlation between applied load and voltage output for calibration with 1 mV (blue), 2.5 mV (red) and 5 mV (green) gain. X-axis shows applied force in Newton and Y-axis shows output voltage.

Initial propulsion measurement: The force measurement results for the initial propulsion measurement are presented in figure 7-10. Figure 7 illustrates crank moment and tangential force as a mean \pm SD for revolution six-nine. The individual ten revolutions representing crank moment and tangential force are presented in figure 8. The propulsion speed for all ten revolutions are illustrated in figure 9.

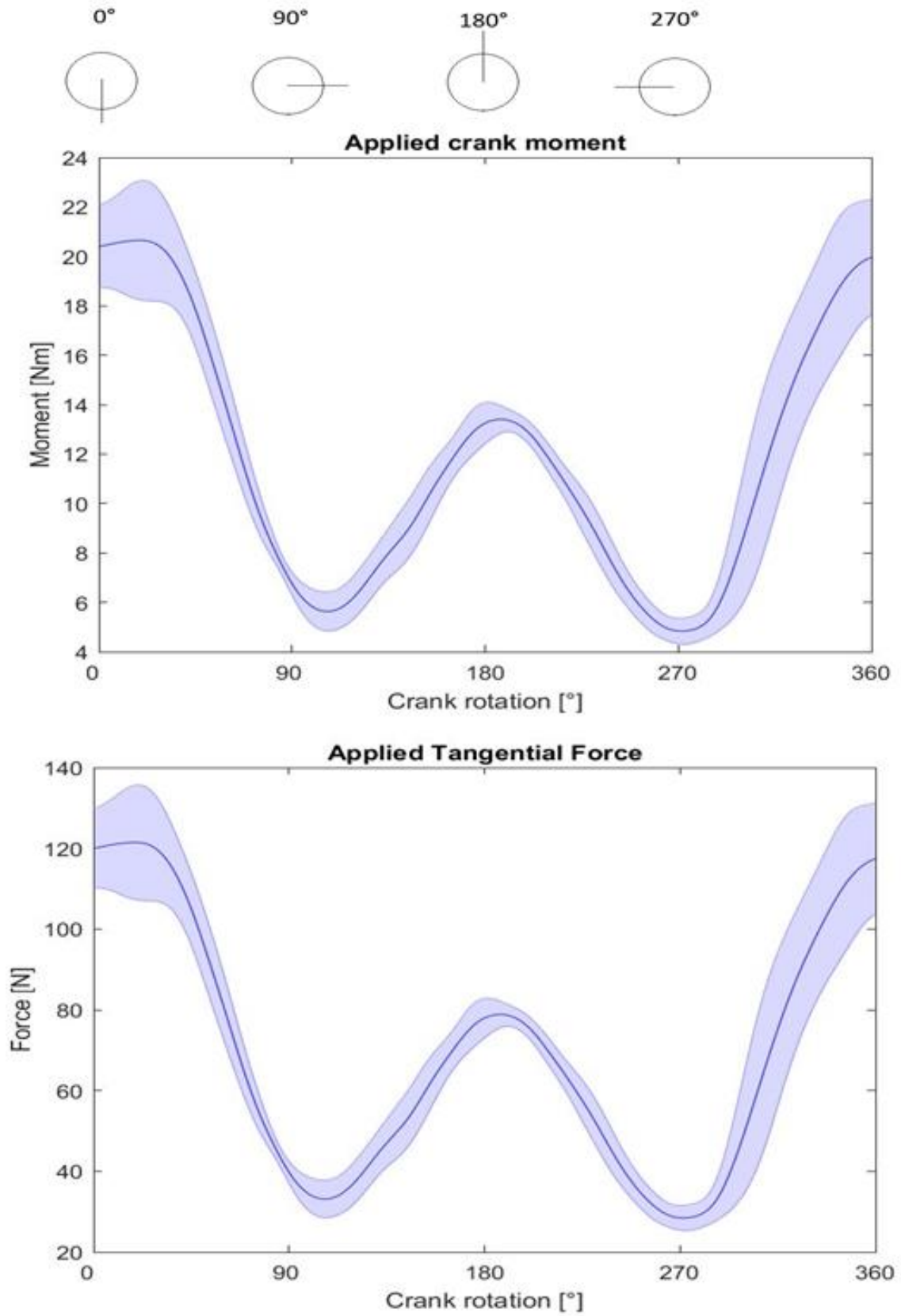


Figure 7 : Average crank moment and tangential force for revolution 6-9 \pm SD, with respect to crank position (0-360°). 0° is represents the position when the pedals are pointing vertically towards the ground.

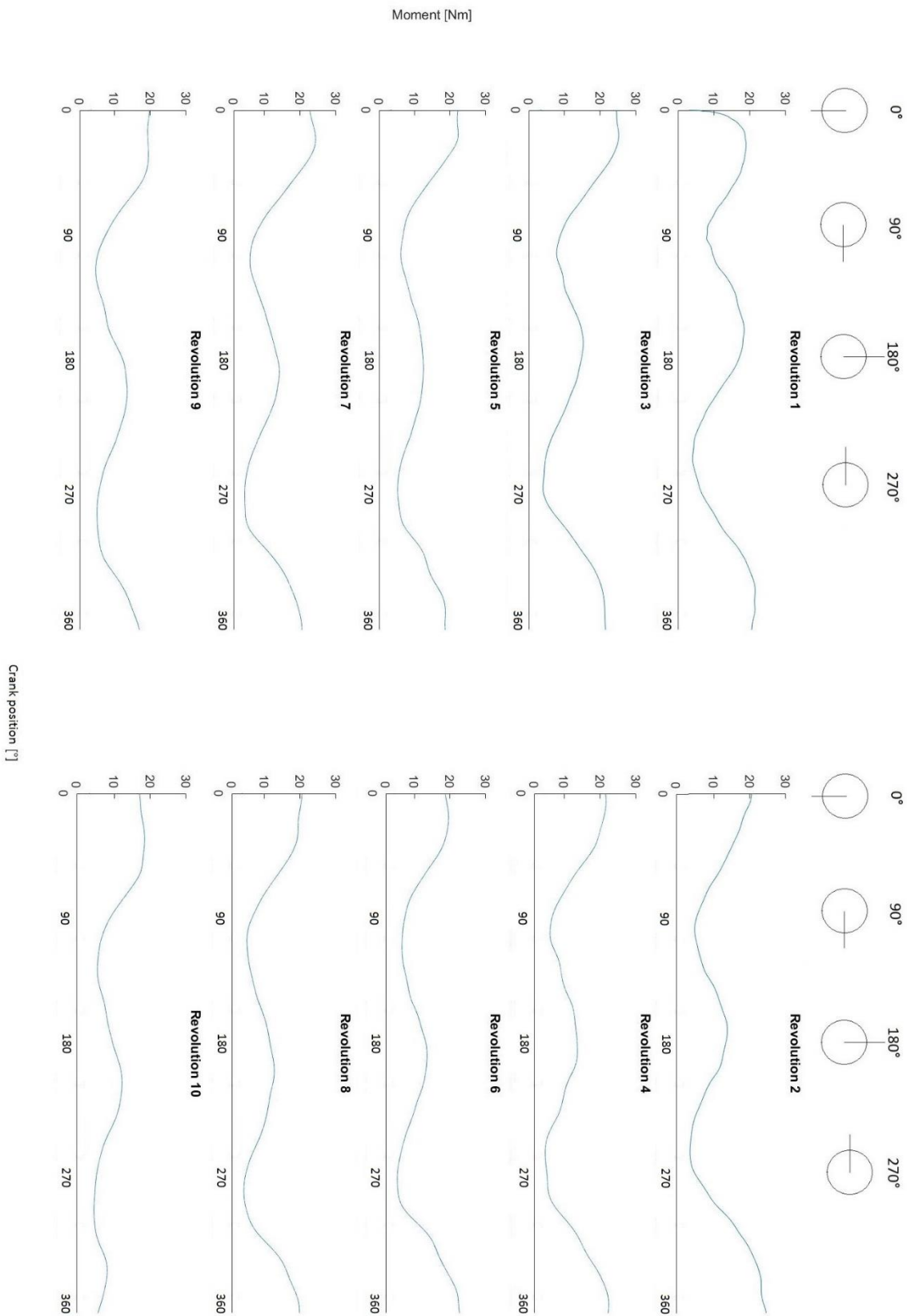


Figure 8 : Applied moment (Nm) for all ten revolutions. 0° is represents the position when the pedals are pointing vertically towards the ground.

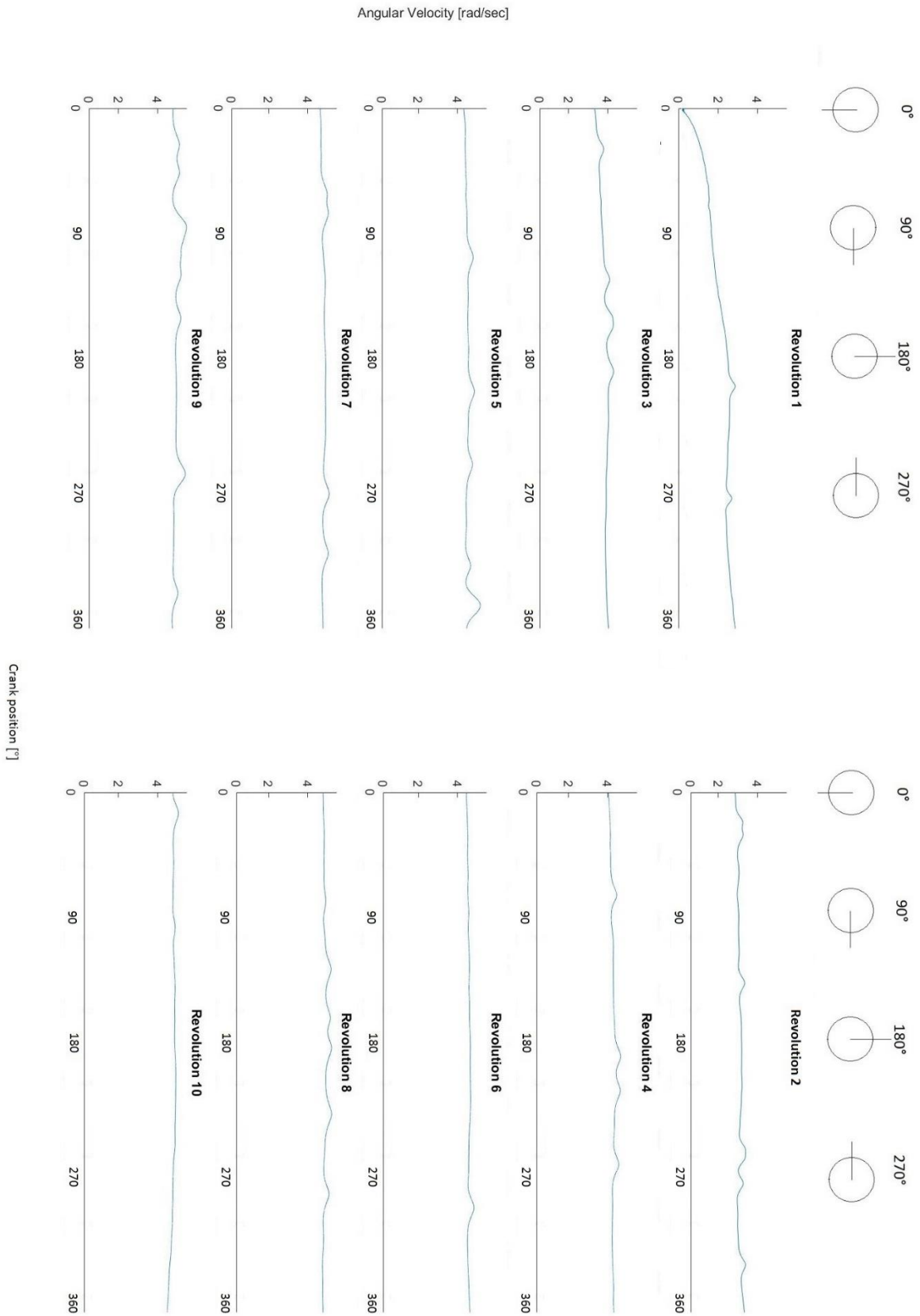


Figure 9 : Angular velocity (rad/sec) for all ten revolutions. 0° is represents the position when the pedals are pointing vertically towards the ground.

Figure 10 illustrates average power production \pm SD with respect to crank position, for revolution 6-9.

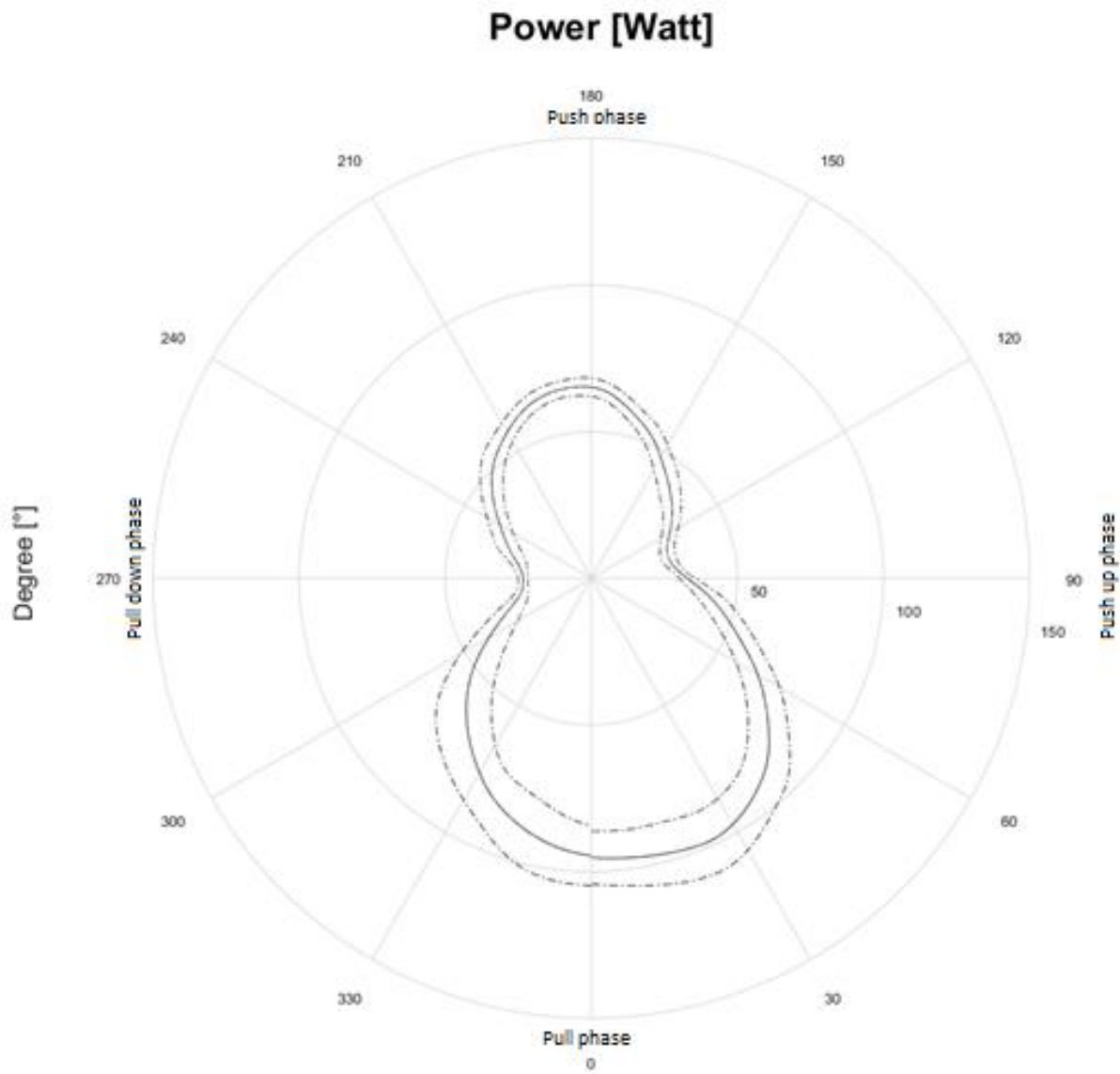


Figure 10 : Average power (watt) for revolution 6-9 (solid line) \pm SD (dashed lines). 0° represents the crank start position when pedals pointing towards the ground 90° with respect to horizontal. The crank revolution is directed counter clockwise.



Discussion

The aim of this paper was to provide technical information on a wireless and relatively inexpensive force measurement system for recumbent hand cycling. The results for accuracy test showed strong coefficients of determination ($R^2=1$) for all three gains. The system is therefore considered valid for measuring tangential force applied to the crankshaft for different gains. The wireless delay test found 4 ms offset, thus the force measurement is slightly delayed in the synchronization with the crank position measurement. This offset was found acceptably low and therefore neglected in the synchronization. The results for angular velocity was lowest in revolution one, due to acceleration in the beginning of the propulsion. However, the velocity was close to constant for the rest of the ten revolutions, with a small velocity increase about 270° and 90°, for some of the revolutions. This suggests a small acceleration when passing the “dead points” appearing about 270° and 90° of the crank cycle.

The pattern for tangential force (figure 7) is similar to the results from the force measurement system developed by Arnet (2012a). Therefore, the system presented in this paper is considered comparable with the system developed by Arnet (2012a), with respect to measuring tangential force in hand cycling. However, the resistance on the home trainer from the initial propulsion measurement in this paper is higher, compared to the treadmill resistance used in the study by Arnet (2012a).

The present system does only measure tangential force contribution from the right arm applied to the crankshaft. Thus, it is assumed that both arms delivers the same force. In addition, the system has no measure of radial and lateral force as the system developed by Arnet (2012a). Hence, the present system does not provide the same detailed force measurement. However, the system is wireless and thereby avoids wire issues when propelling. Simultaneously, the system is applicable for field-testing and not limited to laboratory facilities.

The V-Link®-LXRS® wireless node, applied in this system, has in total seven analog channels and therefore, has the potential for connecting with seven strain gages. This enables the ability to measure force in multiple directions, such as the radial and lateral direction and thus be more comparable to the system developed by Arnet (2012a). However, the sample rate for the V-Link®-LXRS® wireless node decreases when more input sensors are connected (LORD 2015). At the same time, placement of strain gages in the optimal locations can be a difficult task. Therefore, mechanical analysis, such as Finite Element Analysis (FEA) can be performed in order to determine the areas where the greatest strain appears. In order to do so, valid boundary conditions, applied force directions and force magnitudes must be known. Further



development of this wireless system should be concerned with this purpose and so enable the opportunity to measure lateral and radial forces as well.

The participating subject in this study had no previous experience in hand cycling. Therefore, it cannot be excluded that a trained hand-biker would generate another force propulsion pattern. However, as mentioned previous, the tangential force propulsion pattern from the initial propulsion measurement in this paper, is similar to the pattern found by Arnet (2012a) who had a trained hand-biker participating in the study.

With the presented system, it is possible to perform detailed force propulsion measurement, for each crank revolution, which is not possible with currently commercially available power meters. Thus, the system has applicability potential for small handbike manufacturers, in order to undertake quantitative research experiments in the aim of optimizing handbike design.

Conclusion

This technical note introduced a wireless crank moment measurement system, which could determine tangential force and thereby moment applied to the crankshaft of a handbike. This makes it possible to analyze different crank positions (horizontal and vertical position), crank arm lengths, backrest inclination etc. with respect to optimizing propulsion force effectiveness. Futhermore, the system can provide kinetic data as input for serval biomechanical models.

Acknowledgements

The authors of this technical note would like to express our gratitude to John Hansen and Jan Stavnsnøj (Department of Health Science and Technology at Aalborg University) and Søren Brunn and Klaus Kjær (Department of mechanical and manufacturing engineering at Aalborg University) for assisting the manufacturing of the present system.



References

- Arnet, U. 2012a, "Development and validity of an instrumented handbike: initial results of propulsion kinetics", .
- Arnet, U. 2012b, *Handcycling: a biophysical analysis*, Amsterdam: Vrije Universiteit.
- Bafghi, H., A., De Haan, A., Abbasi, Horstman, A., A. & Van, D.W. 2008, "Biophysical Aspects of Submaximal Hand Cycling", *International Journal of Sports Medicine*, vol. 29, no. 8, pp. 630-638.
- Bini, R.R. & Carpes, F.P. 2014, *Biomechanics of Cycling / edited by Rodrigo R. Bini, Felipe P. Carpes*, Elektronisk udgave edn, Cham : Springer International Publishing.
- Faupin, A. & Gorce, P. 2008, "The effects of crank adjustments on handbike propulsion: A kinematic model approach", *International Journal of Industrial Ergonomics*, vol. 38, no. 7, pp. 577-583.
- Garmin , *Garmin Vector Power Meter*. Available: <http://sites.garmin.com/da-DK/vector/> [2016, may].
- Goosey-Tolfrey, V., Alfano, H. & Fowler, N. 2008, "The influence of crank length and cadence on mechanical efficiency in hand cycling", *European journal of applied physiology*, vol. 102, no. 2, pp. 189-194.
- Hoffmann, K. 1989a, "An introduction to measurements using strain gages" in , ed. K. Hoffmann, Darmstadt : Hottinger Baldwin Messtechnik, , pp. 218.
- Hoffmann, K. 1989b, "An introduction to measurements using strain gages" in , ed. K. Hoffmann, Darmstadt : Hottinger Baldwin Messtechnik, , pp. 126.
- Litzenberger, S., Mally, F., & Sabo, A. 2015, "Influence of Different Seating and Crank Positions on Muscular Activity in Elite Handcycling - A Case Study", *Procedia Engineering*, vol. 112, pp. 355.
- LORD, C. 2015, , *V-Link-LXRS Wireless Sensor Node User Manual*. Available: [http://files.microstrain.com/V-Link_User_Manual_\(8500-0006\).pdf](http://files.microstrain.com/V-Link_User_Manual_(8500-0006).pdf) [2016, .
- Quarq , *Quarq Power meters*. Available: <http://www.quarq.com/> [2016, may].
- SRM , *SRM Power meters*. Available: <http://www.srm.de/home/> [2016, may].
- Verellen, J., Theisen, D. & Vanlandewijck, Y. 2004, "Influence of crank rate in hand cycling", *Medicine and science in sports and exercise*, vol. 36, no. 10, pp. 1826.



Biomechanical analysis of hand cycling propulsion movement: A musculoskeletal modelling approach

Frederik Husted Ahlers¹ & Lasse Jakobsen²

Abstract

Objective: Collect experimental data as input for a musculoskeletal model and Implement the data in a musculoskeletal model in order to analyse muscle activity, muscle force and joint reaction forces and moments, during recumbent hand cycling propulsion. **Method:** The kinetic measurement, obtained in this study, was done by using a customized crank moment measurement system. Two Microsoft Kinect one cameras obtained the kinematics of the hand cycling propulsion movement. The kinetics and kinematics founded the input data for a development of a musculoskeletal model, during recumbent hand cycling propulsion. **Results:** Estimation of muscle activity time and muscle force for the prime mover-muscles in the crank cycle were conducted. Simultaneously, the model estimated joint reaction forces and moments. **Discussion:** The model can be applied in studies related to performance optimization and injury prevention in relation to hand cycling.

Keywords: hand cycling, biomechanics, motion capture, musculoskeletal model, handbike

Introduction

Handcycling is mainly popular among paraplegics or otherwise handicapped on lower extremities for handisport (Faupin & Gorce 2008) and as a supplement to the conventional hand-rim wheelchair for transportation (Arnet 2012b). Wheelchair racing at different levels has been related to improved self-esteem and increased social activity for people with disabilities (Cooper 1990), which also has been argued to be valid for hand cycle racers (Zipfel et al. 2009). Handbikes are generally available in four different types; attachment, upright, kneeling and recumbent, dependent on whether it is meant for transport, recreational activity or for Paralympic sport competition respectively (Arnet 2012d). In this study, the focus was on the recumbent edition used for Paralympic sports competition. The recumbent bike is characterized with a low center of mass and a small frontal area, which makes it optimal for sports competition (Cooper 1990).

In relation to Paralympic sports competition, the UCI (international cycling union) has set up five hand cycling disciplines (H1-H5) determined by the athlete's injury severity (UCI). Even though the UCI has set up different competition categories, every athlete is unique with respect to disability, physics and anthropometrics, which sets demands for the hand bike manufacturers in relation to individual customization, weight reduction and interface adjustment possibilities (Zipfel et al. 2009). Therefore, the

¹ frehust@gmail.com - M.Sc Stud. Aalborg University

² lasse@stagsted.net - M.Sc Stud. Aalborg University



handbike interface has received interest in the scientific community (Faupin & Gorce 2008, Arnet 2012c, Litzenberger et al. 2015). Faupin & Gorce (2008) concentrated on crank position with respect to shoulder joint range of motion. Litzenberger et al. (2015) measured surface electromyography (EMG) for the major muscles, during the push phase in the handcycling propulsion cycle, at different seat angles and crank positions. The study investigated none of the major pull muscles on the back. However, the pull propulsion style has been found to be dominant during handcycling (Arnet 2012c). Therefore, the literature seems to lack a full understanding of muscle recruitment pattern for recumbent hand cycling. This can be obtained by using musculoskeletal models, able to estimate muscle activity, muscle force, joint moments and joint reaction forces, which are otherwise difficult to measure, due to invasive procedures (Skals 2015). One of the existing analytical approaches within musculoskeletal modelling is the inverse dynamic approach. Inverse dynamics calculates joint moments based on kinetic and kinematic data in order to estimate muscle activity and muscle force (Damsgaard et al. 2006).

Kinematic and kinetic data are often obtained, by using marker based motion capture systems and force transducers. Unfortunately, marker based motion capture systems and force transducers are often expensive and requires specialized laboratory facilities (Andersen 2013). Hence, research in the field of biomechanical analysis, is limited to universities and/or financially strong companies. However, recent research in the field of cheap marker-less motion capture systems has shown promising validation results (Andersen 2013, Bonnechère et al. 2014, Patrizi et al. 2016).

This leads to the aim of this study, which was two folded 1. Collect experimental input data for an inverse dynamic musculoskeletal model, during recumbent hand cycling, based on low-cost kinematic and kinetic measurements. 2. Implement the input data in a musculoskeletal model for analyzing muscle activity time, muscle force and joint reaction forces and moments. Both aims were conducted as proof-of-concept.

Method and materials

The procedure of this study consisted of two steps:

1. Collect experimental input data for an inverse dynamic musculoskeletal model.
2. Implement the input data in a musculoskeletal model for analyzing purpose.

Subject

One able-body subject (age 26, mass 82 kilograms, height 1.8 m) participated in this study. The subject had no previous experience in hand cycling. Before the experiment, the subject gave his written consent to participate in the study.

Handbike setup

A commercial available handbike was used for this experiment (Racebike model K, Wolturnus, Nibe, Denmark) and connected to KICKR bicycle home trainer (Wahoo Fitness, Atlanta, USA), mounted in a customize upside-down frame (see figure 2). The crank had a horizontal and vertical adjusting ability, which made it possible to suite a wide range of people and meet individual interface preferences. The crank was placed 370 mm vertically to the base plate of the hand bike and 130 mm horizontal with respect to the vertical tube connected to the head tube. The backrest was placed in an angle of 158° with respect to horizontal (see figure 1).

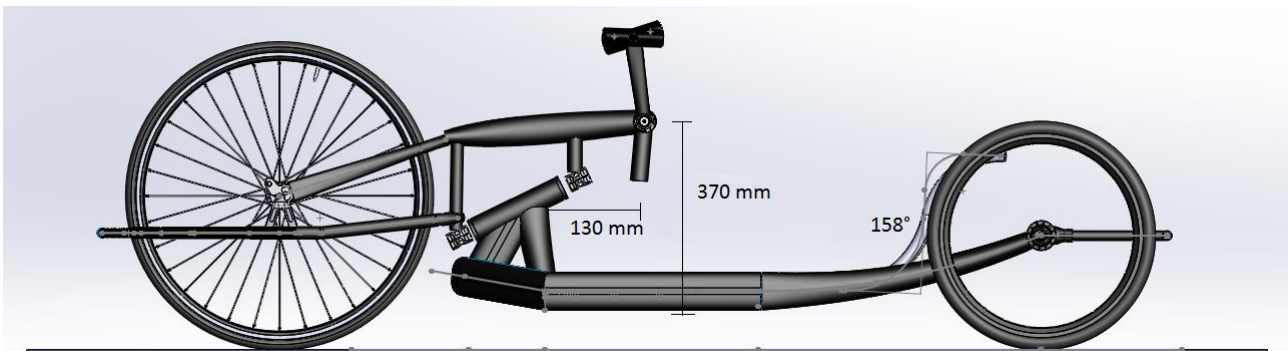


Figure 1 : Handbike setup. Measures of crank position (370 mm vertically to the base plate, 130 mm horizontal with respect to the vertical tube connected to the head tube and backrest angle of angle of 158°)

Experimental data collection

The musculoskeletal model required inputs in terms of human movement kinetic and kinematic. Kinetic is specified as the tangential force applied the crank shaft, whereas kinematic refers to the human propulsion movement.

1.1 Kinetic data collection

The kinetic measurement obtained in this study was done by using a customized force measurement system (Jakobsen & Ahlers, 2016). The force measurement was a strain gage approach and obtained applied crank moment (tangential force applied to the crankshaft). Along with the crank moment measurement, an encoder provided data for crank position and velocity (angular velocity) determination. Technical information regarding the crank moment measurement system is specified in the technical note by Jakobsen & Ahlers (2016).

1.2 Kinematic data collection

Two Microsoft Kinect one cameras (Microsoft, Seattle, USA) were used to capture the hand cycling propulsion movement. The Microsoft Kinect cameras were mounted at two custom-made camera tripods with horizontal and vertical adjusting abilities, in order to ensure optimal field of view. Two computers were running Windows 10 (Microsoft, Washington, USA) and had one USB 3 port each. Simultaneously, both computers were running iPi recorder 3.1.4.43 (iPi Soft, Moscow, Russia) and were connected as a home group via a crossed LAN-cable. Each computer was connected to one Microsoft Kinect camera. In the iPi recorder software one computer was set as master and the second as slave. Hence, the master computer triggered the recording for both Microsoft Kinect cameras simultaneously.

The recordings were processed using iPi Motion Capture Studio 3.2.6.200 (iPi Soft, Moscow, Russia). An “Actor”, scaled to as the subject was manually fitted the cloud representing the subject. The Actor created simultaneously a stick figure of the subject. Subsequent, the “Refit pose” feature were applied and the “Track forward” process automatically tracked the movement. Lastly, “Jitter removal” was applied in order to improve tracking accuracy and reduce noise. The stick figure was exported as a .bvh file.

1.3 Experimental protocol

The subject propelled the handbike with a resistance of 35 %, controlled with the Bluetooth Powered Cycling and Running Workout Tracker 5.7.7 application (Wahoo Fitness, Atlanta, USA), for five minutes as warmup. Subsequently, the subject was asked to flex his elbows at 90° and simultaneously, raise his arms and keep both the upper arm and forearm parallel to the ground, with the palms facing towards the ground and hold the position for five seconds (see figure 2). This was done in order to fit the “Actor” for the subject as described in section 1.2. Next, the subject was asked to grab the handlebars and propelled the bike for 10 revolutions at 35 % with freely chosen speed.



Figure 2 : Experimental setup with handbike connected to home trainer mounted in a customize upside-down frame. The Microsoft Kinect cameras for obtaining kinematic data are located on top of the red camera tripods.

2.1 Musculoskeletal model

The Musculoskeletal model was developed in the AnyBody Modeling System v. 6.0.5 (AMS) (AnyBody Technology A/S, Aalborg, Denmark). The model was based on the “*GaitFullBody*” standard template. Muscles in the lower extremity were excluded since only the upper body extremity provides the propulsion movement in hand cycling. A constant strength muscle model independent of length and contraction velocity muscles was applied and represents the simplest conceivable muscle model (AnyBody tutorial). The model had a total of 27 degrees-of-freedom, including 2x1 DOF at the elbow joint, and 2x3 DOFs at the Glenohumeral joint. The remaining joints and degrees-of-freedom are distributed over the rest of the body, but were not considered as contributing to the propulsion movement.

Motion capture analysis in AMS is traditionally based on maker based motion capture data and cannot apply the iPi stick figure directly from the .bvh file. Hence, a translation from stick figure to marker position was required. This translation refers Andersen’s et al. (2013) work and is illustrated in figure 3. The model was scaled with respect to the stick figure given from the .bvh file (figure 3). The kinematics for the model used the method of Andersen et al. (2009) and minimizes the least-square difference between markers on the model and the stick figure.

Furthermore, the model was constrained with reaction forces in the pelvic and the spine, in order to represent the boundary conditions from the seat and backrest. Additionally, the crankshaft was added as a segment, with the center of the crankshaft being X_0, Y_0, Z_0 (center of green and red coordinate system in figure 4). Two nodes were added ($X \pm 23, Y + 17, Z_0$ with respect to crankshaft center) (blue coordinate systems in figure 4) and represented the two handles. A revolute joint, rotating around x-axis, specified the relation between the crankshaft and the handles. The handles were bounded to the palms in the Z and Y direction.

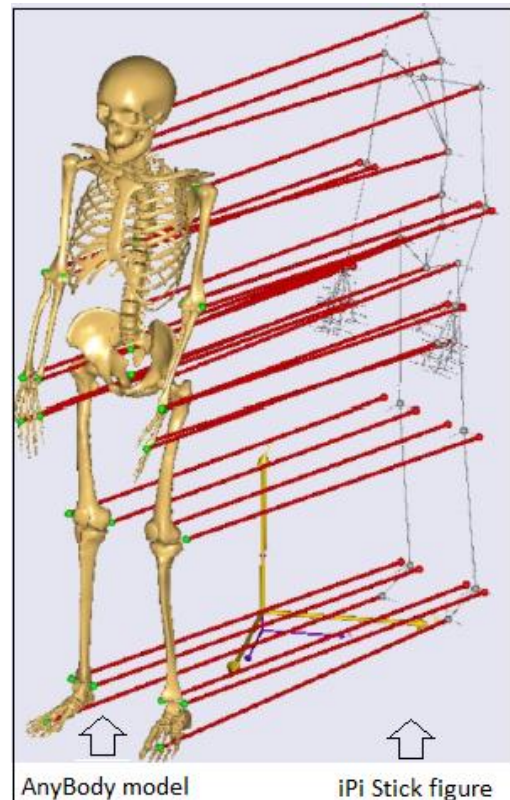


Figure 3 : Translation .BVH stick figure to marker position.

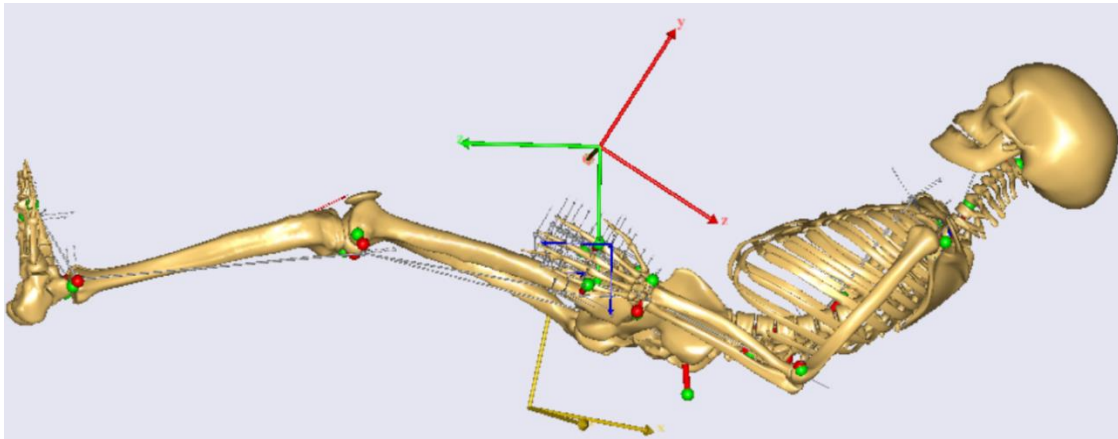


Figure 4 : AMS model of hand cycling subject. The crankshaft is illustrated as the green and red coordinate system. The blue coordinate system represents the handles.

Subsequently, an optimization study was performed with respect to the kinematics of the propulsion movement, in order to determine the crankshaft location and orientation. The revolute joint representing the crankshaft rotated about the x-axis, hence the optimization study optimized the crank position for X,Y,Z and rotation about the Z- and Y-axis.

Last, the kinetic measurement for crank moment was imported for both left and right arm. The kinetic measurement represented force contribution from the right arm and was assumed equal for both arms. The crankshaft moment was applied as a reverse rotation force.

2.2 Data analysis

Estimated muscle force for the following muscles: Biceps, Brachialis, Latissimus Dorsi, Triceps, Pectoralis Major Thoracic, Pectoralis Major Clavicular, Deltoideus anterior, Deltoideus posterior, Infraspinatus and Supraspinatus, were exported. The muscles in the model comprised of several subdivisions, which constitute the different directions of muscle movement. Therefore, all subdivisions for each muscles were summed in order to represent total muscle force. Furthermore, joint moments and reaction forces for the Glenohumeral joint and elbow joint were exported.

Results

All results represents the right side of the upper extremity for revolution seven. The shoulder position is located below the crank and the muscle force, joints moments and joint reaction forces reflects the position illustrated in figure 4. The pull phase was defined as 300°-60°, push up phase 60°-120°, push phase 120°-240° and the pull down phase was 240°-300°.

The kinetic measurement applied for the musculoskeletal model is presented as power (watt) in figure 5. The largest power production appears in the pull phase. The lowest power production appears in the push up phase and pull down phase, when the crank arm is placed horizontal.

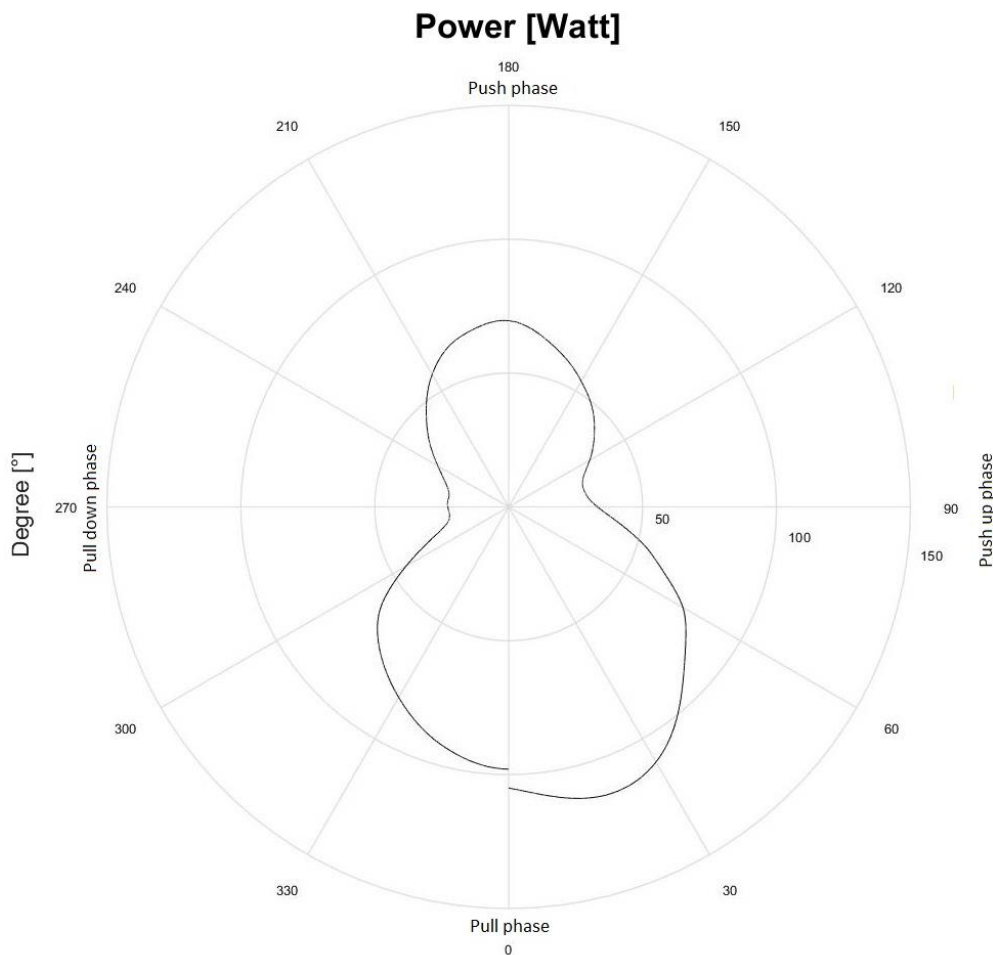


Figure 5 : Power production for revolution seven. The crank revolution is directed counter clockwise. The pull phase is defined as 300°-60°, push up phase 60°-120°, push phase 120°-240° and the pull down phase is 240°-300°.

Muscle activation times are presented in figure 6 for prime movers with respect to crank position.

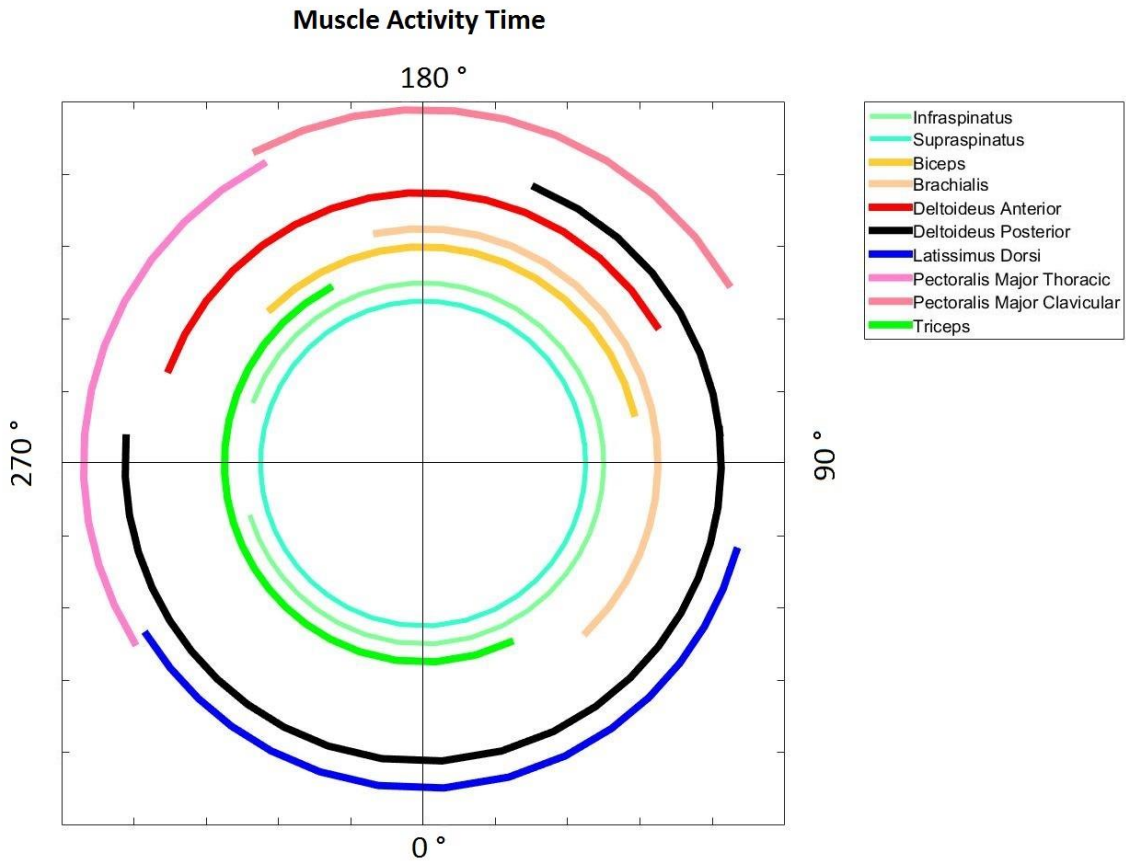


Figure 6 : Muscle activity for right side of upper extremity. Triceps (dark green), Pectoralis Major Clavicular (dark pink), Pectoralis Major Thoracic (light pink), Latissimus Dorsi (blue), Deltoideus Posterior (black), Deltoideus Anterior (red), Brachialis (light yellow), Biceps (dark yellow), Supraspinatus (turquoise) and Infraspinatus (light green), for revolution seven. The crank revolution is directed counter clockwise.

Muscle forces are presented in figure 7-8. Muscle force for the arm muscles are presented in figure 7. Triceps and Brachialis produces large force and acts as antagonists in the propulsion cycle. Muscle force for the trunk muscles are presented in figure 8. Pectoralis Major and Latissimus Dorsi acts as antagonists. However, infraspinatus produces the largest force.

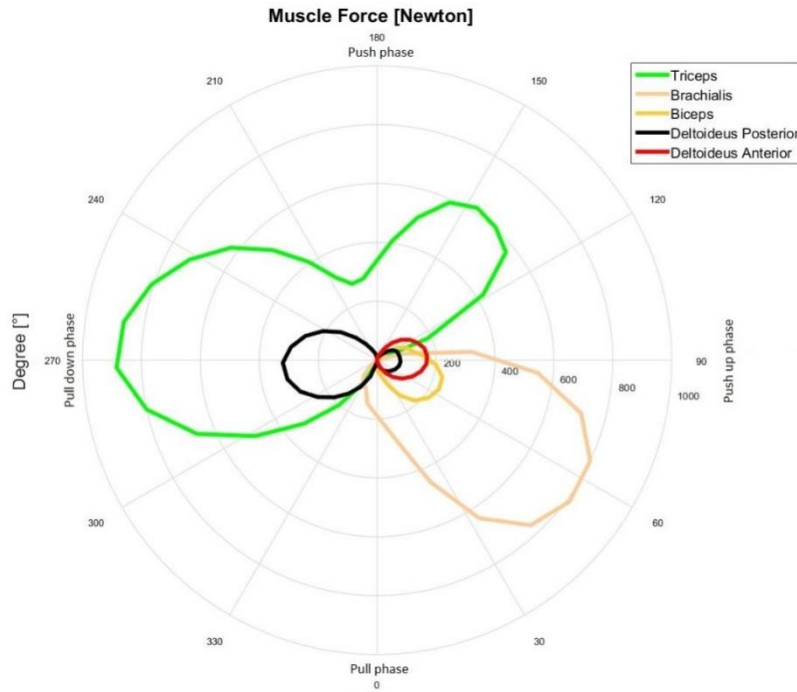


Figure 7 : Muscle force for right arm muscle. The crank revolution is directed counter clockwise.

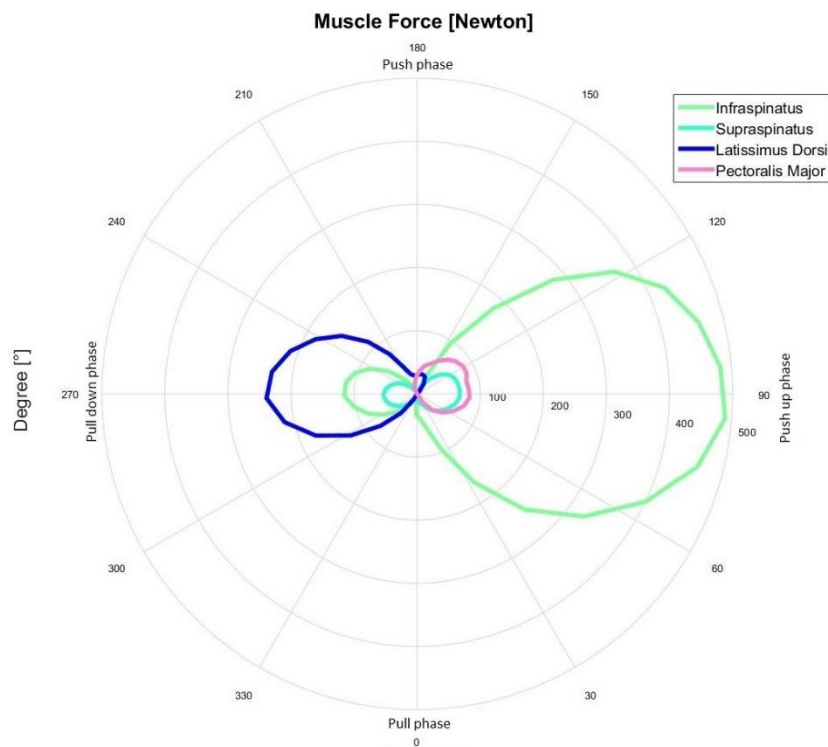


Figure 8 : Muscle force for trunk muscle. The crank revolution is directed counter clockwise.



Elbow- and Glenohumeral joint moments are illustrated in figure 9. Flexion for the Glenohumeral- and elbow joint produces the largest moment. Elbow pronation was found to contain the lowest moment.

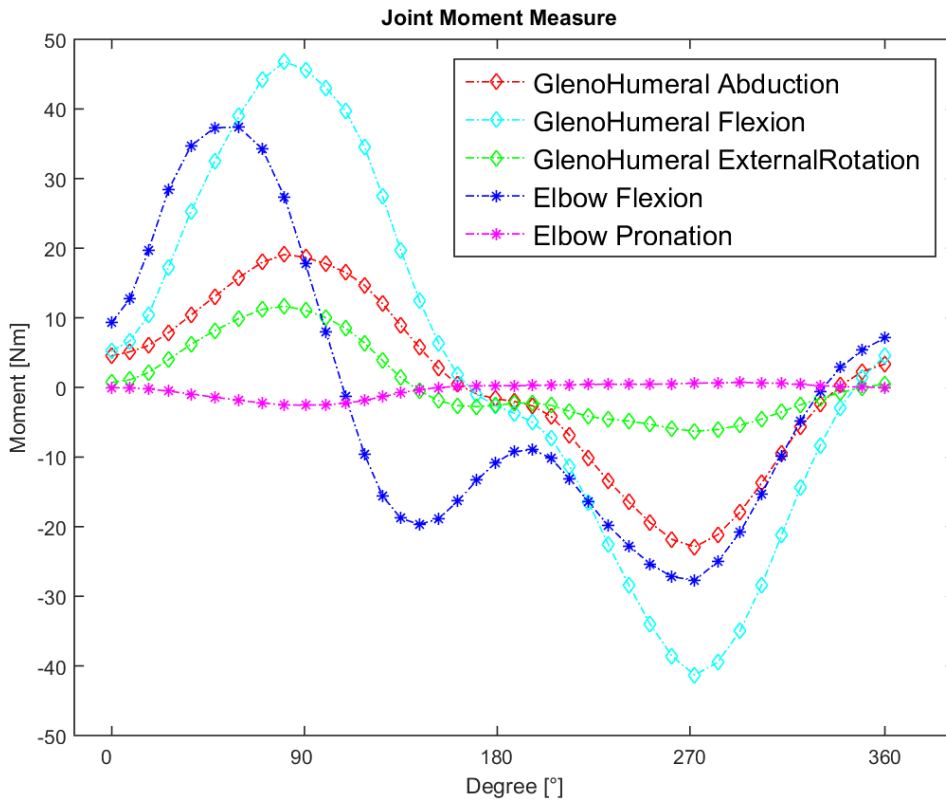


Figure 9 : Moments (Nm) for the Glenohumeral- and elbow joint with respect to crank position. 0° represents the crank start position when pedals pointing towards the ground 90° with respect to horizontal.

Reaction forces for the Glenohumeral joint appears in figure 10. All the forces seem to peak around 90° and 270°, when the crank arms are horizontally located.

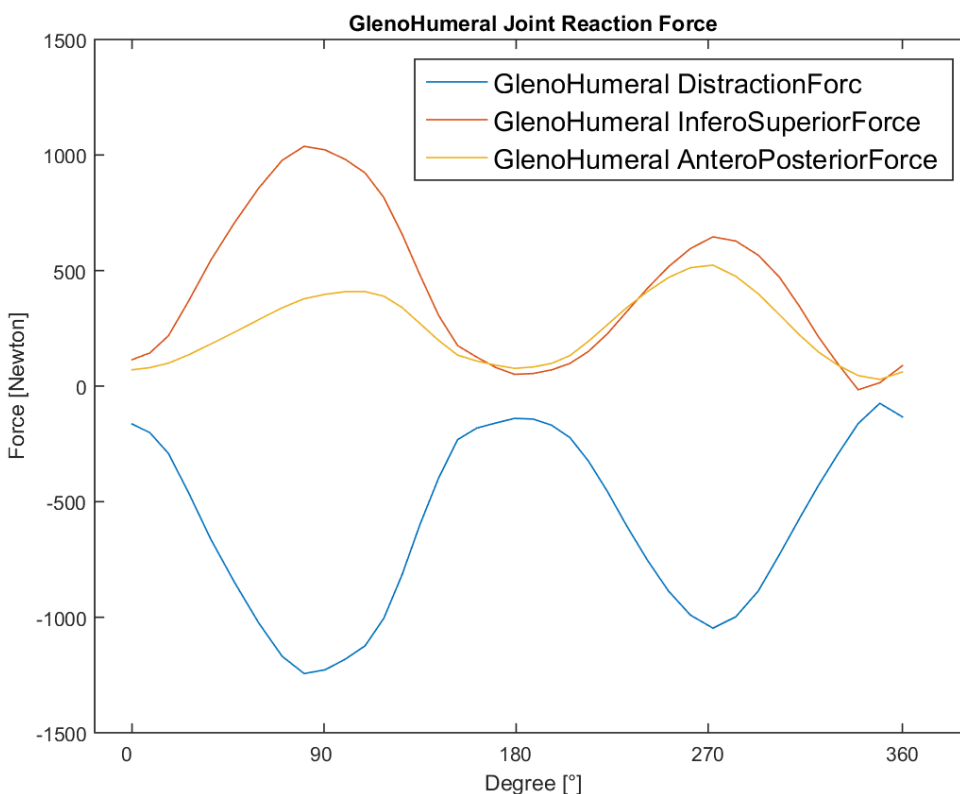


Figure 10 : Glenohumeral joint reaction force with respect to crank position. 0° represents the crank start position when pedals pointing towards the ground 90° with respect to horizontal.



Discussion

The pull phase in the propulsion cycle was found to be dominant for power production (see figure 5). This is in accordance with previous findings for submaximal hand cycling propulsion (Arnet 2012c). The results for joint moments (figure 9) illustrates a higher flexion moment for the Glenohumeral joint compared to the elbow joint. Joint moment are produced by muscles working across the joint, which suggest higher demands for the muscles working across the Glenohumeral joint compared to the muscles working across the elbow joint. This is in correlation with the relatively high muscle force found for Triceps, working as agonist to Latissimus Dorsi (see figure 7 and 8) for extension of the Glenohumeral joint in approximately 270° of the crank cycle. Muscle force for Infraspinatus reaches peak force in approximately 90° of the crank cycle and is properly due to eccentric muscle work in order to stabilize the Glenohumeral joint. The muscle activation time shown in figure 6 is similar to the muscle activation time found with EMG measurement by Litzenberger et al. (2015) for triceps and biceps. Pectoralis Major in this study is active prior in the crank cycle compared to Pectoralis Major in the study by Litzenberger et al. (2015). Deltoideus in this study is divided into an anterior and posterior part and is therefore difficult to compare with Deltoideus activation in the study by Litzenberger et al. (2015), since the anterior/posterior positioning of the EMG electrode is not specified. Litzenberger et al. (2015) had no measure for Latissimus Dorsi, which therefore cannot be compared. In addition, the muscle activation time for infraspinatus and supraspinatus presented in this study is difficult to measure with EMG, due to in vivo placement of the electrodes. The limitations of EMG measurements makes musculoskeletal model prediction of muscle activity and joint reaction force valuable. The Glenohumeral distraction force reaches 1243 N and 1047 N in the pull down and push up phase respectively. The Glenohumeral distraction force has been acknowledge as a risk factor for developing of shoulder injuries (Stuelcken et al. 2010, Werner et al. 2006). Therefore, minimization of the Glenohumeral distraction force potentially minimize the injury risk in hand cycling. However, the Glenohumeral distraction force, found in this study for hand cycling, is more than twice as high compared to explosive cricket fast bowling movement (Stuelcken et al. 2010). Therefore, the results for Glenohumeral distraction force found in this study must be interpreted with caution.

A challenge arises in the AnyBody model segment scaling, when applied paraplegics or lower limb amputees due to abnormal body mass proportions. The model scales body segments with respect to total body mass, which for paraplegics or lower limb amputees can be a poor assumption, due to significant reduced muscle size or leg absence. Thus, the models assumed maximum muscle strength in the upper extremity could be lower, compared to reality. Therefore, muscle activity, which is a percentage of



maximum muscle activity, may be a poor measure for this musculoskeletal model, when applied paraplegics. Instead, muscle force is recommended as measure for muscle work.

The Microsoft Kinect cameras applied in this study as motion capture system is a low-cost solution compared to traditional marker based motion capture systems. Therefore, the kinematic quality of the Kinect cameras can be expected to be of minor quality, compared to high-end marker based motion capture system. A study validated the Microsoft Kinect 360 camera (first version) with a marker based system and found good correlation for shoulder abduction, but less accuracy for elbow flexion and lower extremity movements (Bonnechère et al. 2014). However, the Microsoft Kinect one camera used in this study, has underwent several improvements compared to Microsoft Kinect 360, including five additional joint determinations in the upper body for improved tracking accuracy (Microsoft corporation. 2016). Further studies in relation to Microsoft Kinect one camera validation must clarify the exact accuracy.

This study presents a model able to predict muscle activity time, muscle force, joint reaction forces and joint moments, for the propulsion cycle, during recumbent hand cycling. This musculoskeletal model approach and results provides the base for study opportunities related to interface setup, in order to minimize injury risk. E.g. for calculation of Glenohumeral contact force, which previously has been found to be an injury risk for wheelchair handrim propulsion and hand cycling (Arnet 2012a). Furthermore, the model can be applied in studies related to performance optimization, aimed to lowering muscle activity or enhance force production for selected muscles, by changing the handbike interface setup. Research in the aforementioned fields can provide handbike design guidelines for handbike manufactures, whether suited for minimizing injury risk or performance enhancement.

Conclusion

This study presented a human musculoskeletal model during hand cycling propulsion in a recumbent handbike. The model was able to predict muscle activity time, muscle force, joint moments and joint reaction forces. Furthermore, this study presented a novel and low cost method for obtaining kinematic and kinetic data as input for the musculoskeletal model. Due to the low cost method for obtaining kinematic and kinetic data, this study suggested a research opportunity for handbike designers and manufactures.



Acknowledgements

The authors of this study expresses gratitude to Michael Skipper Andersen for assisting the setup of the musculoskeletal model. Furthermore, we addresses our gratitude to Wolturnus A/S for providing the handbike used in this study.

References

- Andersen, M.S., Damsgaard, M. & Rasmussen, J. 2009, "Kinematic analysis of over- determinate biomechanical systems", *Computer methods in biomechanics and biomedical engineering*, vol. 12, no. 4, pp. 371-384.
- Andersen, M.S. 2013, "Full-body musculoskeletal modeling using dual microsoft kinect sensors and the anybody modeling system", , pp. 23-24.
- AnyBody, T.A. *AnyBody tutorial - muscle modeling - lesson 5*, AnyBody Modeling System v. 6.0.5 edn.
- Arnet, U. 2012a, *Handcycling: a biophysical analysis Chapter 4*, Amsterdam: Vrije Universiteit.
- Arnet, U. 2012b, *Handcycling: a biophysical analysis Chapter 5*, Amsterdam: Vrije Universiteit.
- Arnet, U. 2012c, *Handcycling: a biophysical analysis Chapter 6*, Amsterdam: Vrije Universiteit.
- Arnet, U. 2012d, *Handcycling: a biophysical analysis Chapter 7*, Amsterdam: Vrije Universiteit.
- Bonnechère, B., Jansen, B., Salvia, P., Bouzahouene, H., Omelina, L., Moiseev, F., Sholukha, V., Cornelis, J., Rooze, M. & Van, S.J. 2014, "Validity and reliability of the Kinect within functional assessment activities: Comparison with standard stereophotogrammetry", *Gait & posture*, vol. 39, no. 1, pp. 593-598.
- Cooper, R.A. 1990, "Wheelchair racing sports science: a review", *Journal of rehabilitation research and development*, vol. 27, no. 3, pp. 295.
- Damsgaard, M., Rasmussen, J., Christensen, S., Surma, E. & de Zee, M. 2006, "Analysis of musculoskeletal systems in the AnyBody Modeling System", *Simulation Modelling Practice and Theory*, vol. 14, no. 8, pp. 1100-1111.
- Faupin, A. & Gorce, P. 2008, "The effects of crank adjustments on handbike propulsion: A kinematic model approach", *International Journal of Industrial Ergonomics*, vol. 38, no. 7, pp. 577-583.
- Jakobsen, Lasse & Ahlers, Frederik Unpublished technical note 2016, "Development of a wireless crank moment measurement-system for handbike: Initial results of propulsion kinetics".
- Litzenberger, S., Mally, F., & Sabo, A. 2015, "Influence of Different Seating and Crank Positions on Muscular Activity in Elite Handcycling - A Case Study", *Procedia Engineering*, vol. 112, pp. 355.



- Microsoft, corporation. 2016 , *Kinect hardware*. Available: <https://developer.microsoft.com/en-us/windows/kinect/hardware>.
- Patrizi, A., Pennestrì, E. & Valentini, P.P. 2016, "Comparison between low- cost marker- less and high- end marker- based motion capture systems for the computer- aided assessment of working ergonomics", *Ergonomics*, vol. 59, no. 1, pp. 155-162.
- Skals, S.L. 2015, *Prediction of ground reaction forces and moments during sports-related movements*.
- Stuelcken, C.M., Ferdinands, R.E.D., Ginn, K.A. & Sinclair, J.P. 2010, "The Shoulder Distraction Force in Cricket Fast Bowling", *Journal of Applied Biomechanics*, vol. 26, pp. 373.
- UCI *UCI cycling regulations*
Part 16 para-cycling
(version on 1.02.14), http://www.uci.ch/mm/Document/News/Rulesandregulation/16/26/73/16hand_E_English.PDF.
- Werner, S.L., Jones, D.G., Guido, John A., Jr, & Brunet, M.E. 2006, "Kinematics and kinetics of elite windmill softball pitching", *The American Journal of Sports Medicine*, vol. 34, no. 4, pp. 597.
- Zipfel, E., Olson, J., Puhlman, J. & Cooper, R.A. 2009, "Design of a custom racing hand- cycle: Review and analysis", *Disability & Rehabilitation: Assistive Technology*, 2009, vol. 4; Vol.4, no. 2; 2, pp. 119; 119-128; 128.



Biomechanical analysis of hand cycling
propulsion movement. A musculoskeletal
modelling approach

&

Development of a wireless crank moment
measurement-system for a handbike: Initial
results of propulsion kinetics

WORKSHEETS

Lasse Jakobsen & Frederik Husted Ahlers

3/6/2016



Table of contents

1	Contents	
2	Background	3
2.1	Handbike history.....	3
2.2	Handbike user-interface	3
2.3	Hand bike setup	4
2.4	Movement analysis of hand cycle locomotion	5
2.5	Musculoskeletal modelling.....	6
2.6	Anybody modelling system (AMS).....	6
3	Biomechanical analysis system - solution strategy	7
3.1	Requirements.....	7
4	Kinematic measurement	8
4.1.1	Requirements.....	8
4.1.2	Microsoft Kinect one camera	8
4.1.3	iPi soft motion capture	9
4.1.4	Design.....	9
5	Kinetic measurement.....	10
5.1.1	Requirements.....	10
5.2	Strain gage force measurement	11
5.2.1	Design	11
5.3	Crank position measurement	13
	Requirements.....	13
5.3.1	Design	13
6	System implementation	16
6.1	Parameter identification –motion capture to musculoskeletal model	16
6.2	Calibration procedure.....	18
7	References.....	20

2 Background

In the following, the fundamental information regarding the procedures associated with the two articles is presented, by providing an overview of the handcycling sport discipline and a theoretical examination of the applied hardware and software.

2.1 Handbike history

The first reported handbike was developed by a watch-maker called Stephan Farfler back in the 1655, who redesigned a wooden wheelchair into a handbike with a crank and gearwheel (Hettinga et al. 2010). Along with the development of technology, handbikes were suited with tires and chains and in the middle of 20th century handbikes got an asynchronous propulsion crank. However, modern handbikes are mostly equipped with synchronous cranks. (Arnet 2012b). The synchronous propulsion has by several researchers been found to be preferable with respect to mechanical efficiency, peak power output and steering abilities. ((Arnet 2012b, Abel et al. 2003, Dallmeijer et al. 2004)). Thus, the synchronous crank is applied in most modern handbikes. Figure 1 illustrates a Synchronous and asynchronous crank.

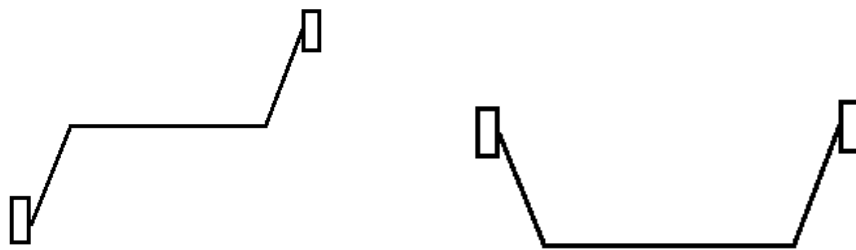


Figure 1: Asynchronous crank (to the left) and synchronous crank (to the right)

In 2014 hand cycling became part of the Paralympics for the first time (Arnet 2012b). Hereafter, hand cycling has become a popular sport and recreational activity for leg amputee and able-bodied people (Hettinga et al. 2010).

2.2 Handbike user-interface

The handbike user-interface has been under investigation by several researchers (Arnet 2012b) (Faupin, Gorce 2008, Litzberger, Mally & Sabo 2015). In order to produce the most power and be most energy efficient, an optimal handbike user-interface is preferred by athletes. Arnet et al. (2012) proposed a model illustrating the factors influencing the power output (PO), when riding a handbike (Figure 2).

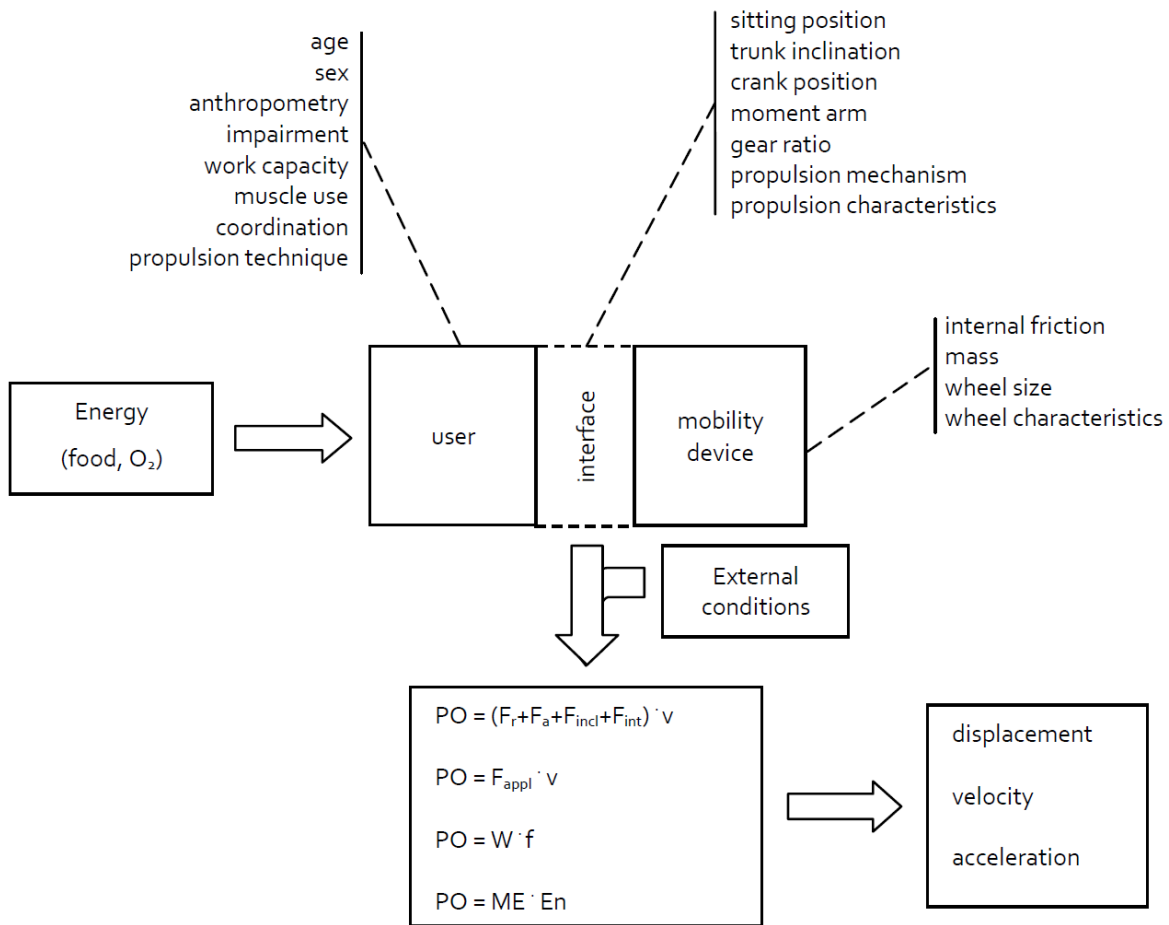


Figure 2: Handbike user interface factors, influencing the power output (PO) - Arnet et al. (2012)

This includes factors related to the user, interface and mobility device (the handbike). Hence, the power output is influenced by several factors.

2.3 Hand bike setup

The sitting posture on a handbike depends on the purpose. For tour rides, more upright trunk posture is observed (See figure 3). For some handbike types, the trunk can be involved in power production by bending the trunk forward during the push-phase. This method is limited to users with their abdominal and extensor muscles functioning (Zipfel et al. 2009).

For competition rides, the aerodynamics associated with small frontal plane is an important factor because of the high speed and the air resistance. Therefore, recumbent bikes with low frontal area and a low sitting position are mostly preferred for competition. However, the reclined position handbike is not necessarily the optimal position for maximal muscle work, but a compromise between aerodynamics and physical performance (Hettinga et al. 2010).

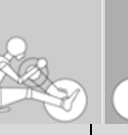
AP	AP1	AP2	AP3	ATP	ATP1	ATP2	ATP3
Arm-power				Arm-Trunk-Power			
Wheelchair-sit	Recumbent 60°	Recumbent 30°	Recumbent 0°	Wheelchair-sit	Car-seat	Long-seat	Knee-seat
upright	Reclined	Reclined	Reclined	forward	Forward	Forward	Forward
Attach-unit	Rigid frame	Rigid frame	Rigid frame	Attach-unit	Rigid frame	Rigid frame	Rigid frame
							
100%	62,6%	39,6%	33,3%	96,8%	82,8%	60,9%	60,3%
Tour	Tour	competition	Competition	Tour	tour	Competition	competition
		HC-A,-B,C1	HC-A,-B,C1			HC-C1	HC-C2

Figure 3: Different hand bike types and classifications. (Hettinga et al. 2010)

2.4 Movement analysis of hand cycle locomotion

In order to determine which muscles and joints to analyze in the musculoskeletal model, a movement analysis of the involved body segments is performed in the following. Since the major movement pattern are related to the arms a simple model of the joints and degrees of freedom in the arms are illustrated in figure 4 (Faupin, Gorce 2008).

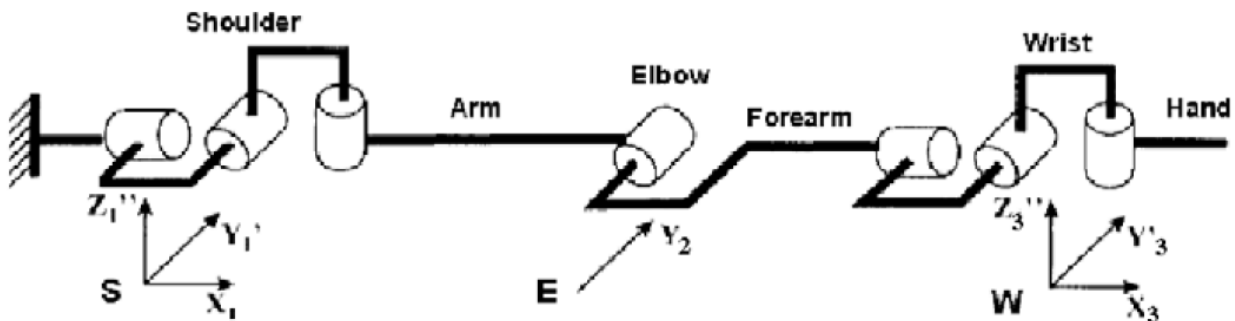


Figure 4: Arm and joints model (Faupin, Gorce 2008).

Hence, the shoulder is a spherical joint with three degrees of freedom, the elbow is a revolute joint with one degree of freedom, the forearm is a swivel joint with one degree of freedom and the wrist is a radiocarpal joint with two degrees of freedom. These sums up to seven degrees of freedom for each arm. Therefore, the model can predict the muscles involved, muscle force, joint reaction forces and moments related to the three joints.



2.5 Musculoskeletal modelling

Computer simulation of physical movement has revolutionized the knowledge of the internal forces acting inside the human body and the interaction between human and environment. Computer-aided engineering (CAE) got a long history and today almost every physical phenomenon can be simulated (Lund et al. 2012). Biomechanical simulations perceives the human body as a mechanical system composed of rigid bodies. Musculoskeletal modelling is an analytical tool, able to simulate internal behaviors in the human body, which otherwise is very difficult to measure by experimental setup. The analytical approach is driven by the equation of motion, which provides relationship between motion and forces in a mechanical system. The equation can be solved in two ways, either by a forward dynamic analysis or by an inverse dynamic analysis (Damsgaard et al 2006). The purpose of forward dynamic analysis is to calculate the movement of the system by knowing the forces acting within the system, whereas inverse dynamics calculates the forces acting within the system by knowing the movement of the system. In the present thesis, an inverse dynamic approach were performed in the AnyBody Modeling System v. 6.0.5 (AMS) (AnyBody Technology A/S, Aalborg, Denmark).

2.6 Anybody modelling system (AMS)

If the motion of the mechanical system is known, along with the forces and boundary conditions, then the equation of motion provide the internal forces (Vaughan, Davis & Coonor 1999, Rasmussen, Damsgaard & Voigt 2001). However, the musculoskeletal model in AMS is statically indeterminate, because there are more available muscles than needed to produce a given motion. The AMS solve this problem by implementing the rational criterion, which is based on the principle that the central nervous system recruits the muscles that makes the desired movement with minimum effort (Rasmussen, Damsgaard & Voigt 2001).

As mentioned previously, the movement has to be known to conduct an inverse dynamic analysis and the object is to calculate the moments and forces based on the movement. To solve the dynamics of the handbike motion with AMS, different parameters have to be known: 1) the body segment parameter - segment mass, centre-of-gravity and moment-of-inertia, are estimated by the mass and height of the subject. 2) Each segment kinematics. 3) The external forces acting on the body (Vaughan, Davis & Coonor 1999). The AMS can solve the inverse dynamic with only the kinematics, a so-called top-down approach, but this approach is sensitive to uncertainties in the data. This can lead to misreading of the joint moments (Riemer, Hsiao-Weckler 2008). By adding external forces, the bottom-up approach is possible, which involves

measurements of external forces acting on the first segment, this approach is less sensitive to uncertainties

in the kinematics (Riemer, Hsiao-Weckslar 2008). When adding external forces the inaccuracies caused by the acceleration inputs will be reduced. Therefore, the joint moment predictions tend to be more accurate in the contact part of the multibody system. (Riemer, Hsiao-Weckslar 2008)

3 Biomechanical analysis system - solution strategy

The purpose of this thesis was to present a biomechanical analysis of the hand cycling propulsion movement. This was done with an inverse dynamic approach in the human musculoskeletal modeling system AnyBody v. 6.0.5 (AMS) (AnyBody Technology A/S, Aalborg, Denmark). In order to drive an inverse dynamic musculoskeletal model, a system able to capture human movement kinematics and kinetics was required. The system must meet the following requirements:

3.1 Requirements

- Kinematics of hand cycling propulsion movement (motion capture)
- Kinetics of hand cycling propulsion movement (moment applied the crank)
- Crank position and velocity in order to synchronize kinematics and kinetics and for power calculation

A model of the system solution is presented in figure 5.

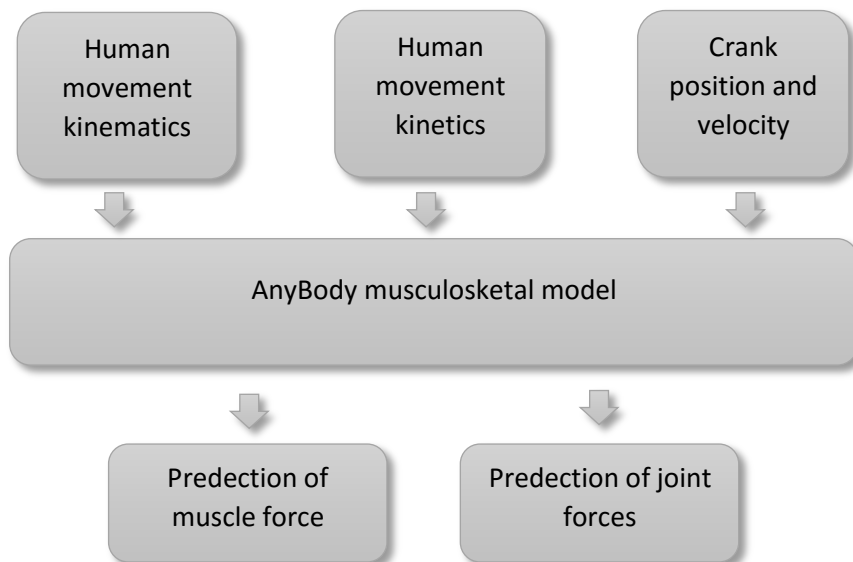


Figure 5: System solution model.

The system must be suited for use by smaller companies, concerned with handbike design and manufacturing. Hence, it must be relatively inexpensive, quick to setup and mobile. Thus, expensive research equipment such as immobile marker-based motion capture systems, six degrees of freedom force transducers suited with heavy connection wires and large laboratory facilities are not well suited for this



system. Instead, a system composed of two Microsoft Kinect One cameras, as motion capture system along with a wireless strain gage setup, mounted on the crankshaft, will provide the kinematics and kinetics needed to drive the musculoskeletal model. An optical wheel encoder setup on the crank will contribute with the crank position and speed information, needed to synchronize the kinematics and kinetics and for calculation of power. The specific requirements for each subpart of the system are established in the following chapters, in order to provide acceptable measurement quality. Hereby, theoretical background and considerations for the applied sensors/measurement equipment are presented.

4 Kinematic measurement

Multiple methods for obtaining kinematic or movement data exists and vary widely in complexity, costs and accuracy (Skals 2015). Currently, the golden standard of motion capture include marker-based systems (MBS), with reflective bone-pin studies along with infrared cameras (Benoit et al. 2006). However, bone-pin studies requires invasive bone attachment and are therefore rare. Furthermore, the infrared camera system is very expensive and requires large laboratory facilities. As counterpart, newly developed markerless systems (MLS) seem promising for biomechanical analysis and are much more affordable and relatively mobile (Bonnechère et al. 2014). As the MLS are concerned with the boundaries of the human body, it is less accurate compared to some of the MBS. However, research in this field is ongoing and continues to improve in order to overcome the technical issues (Zhou, Hu 2008).

4.1.1 Requirements

- Markerless motion capture
- Adjustable to fit view of interest
- Portable

4.1.2 Microsoft Kinect one camera

The Kinect camera (see figure 6) is a cheap solution for MLS and was found appropriate for this system in relation to kinematic measurement. It was originally developed for movement based console games for Microsoft X-box (Microsoft, Seattle, USA). However, the Kinect-technology is also interesting in the research field of forensics, robotics, mapping and 3D human modeling (Khoshelham 2012) (Andersen 2013). The camera is basically made up of an laser emitter, RGB (red green blue) camera and an infrared camera. The frame rate is 30 frames per second and consists of depth and color images simultaneously. The combination of depth and images results in a point cloud. The emitter transmits a light pattern onto an object and the infrared camera captures the light pattern and compares it with a reference pattern in its memory, which makes it able to detect depth and movement (Khoshelham 2012).



Figure 6: Picture of Microsoft Kinect one camera.

4.1.3 iPi soft motion capture

The iPi soft motion capture is a tracking software, which uses a tracking algorithm to create a human stick figure from the human point cloud, gathered from the Microsoft Kinect camera. The iPi software is separated into a recorder-program and a mocap studio-program. The recorder-program is able to connect up to four separate Microsoft Kinect one cameras dependent on the license.

4.1.4 Design

Two Microsoft Kinect one cameras were used to capture the hand cycling propulsion motion and the iPi soft 3.1.4.43 computer software (iPi soft, Russia) was used as the motion capture software. The Kinect one camera were originally developed for Microsoft X-box one, hence a USB converter is needed for computer connection. Two computers were running Windows 10 (Microsoft, Washington, USA) and had one USB 3 port each. Simultaneously, both computers were running iPi recorder 3.1.4.43 (iPi Soft, Moscow, Russia) and were connected as a home group via a crossed LAN-cable. Each computer was connected to one Kinect camera. In the iPi recorder software one computer was set as master and the second as slave. Hence, the master computer triggered the recording for both Kinect cameras simultaneously.

Two custom-made camera tripods were designed and manufactured, in order to create a flexible system able to orient and locate the Microsoft Kinect cameras in multiple directions. The flexibility erupts by telescope poles in both the horizontal and vertical axes (See figure 7). The tripods consisted of seven parts, made of aluminum and plastics. The tripods are considered portable. The technical drawings for manufacturing are located in appendix.



Figure 7: Custom-made adjustable microsoft kinect camera tripods.

5 Kinetic measurement

Several sensor technologies such as capacitive sensors, piezoelectric sensors and strain gage sensors are available in order to measure kinetics. The choice of sensor depends on the exact purpose, required accuracy, sample rate and price. Common for the majority of the sensor technologies, is the ability to measure electrical resistance change when the sensors are submitted to strain. Most studies concerned with biomechanical analysis of human movement, obtains kinetic measurement by using strain gage based force platforms or force transducers. (Neuman 2000). However, measuring kinetics of moving/rotating objects requires a strategy in order to avoid conflicting with wires. Thus, novel wireless systems is commercially available and enables the ability to measure kinetics at moving/rotating objects.

5.1.1 Requirements

- Measure crank moment (tangential force applied to the pedals during the hand cycling propulsion movement)
- Sample at least 20 HZ in order to detect the changes in force for one propulsion cycle (The minimum sampling rate is based on the force measurement characteristics when propelling a handbike with 60-70 rmp, obtained by Arnet et al (2015) and accounts for Nyquist minimal sampling rate (Arnet 2012a)).

- Sample wirelessly in order to avoid entangling wires with the crank, when propelling and resemble realistic hand cycling.

5.2 Strain gage force measurement

A strain gage is a device able to measure normal strain on a surface. It consists of a metal wire folded into a grid, which is bonded to a surface of an object, thus the strain of the object is transferred to the strain gage. A strain gage measures changes in electrical-resistance when it is strained, whether it elongates or compresses. The electric resistance is converted into a measurement of strain and can only measure strain in one direction. Therefore, more strain gages in different directions are needed in order to determine strain in different directions. Three strain gages in three directions are illustrated in figure 8. (Gere, Goodno 2013)

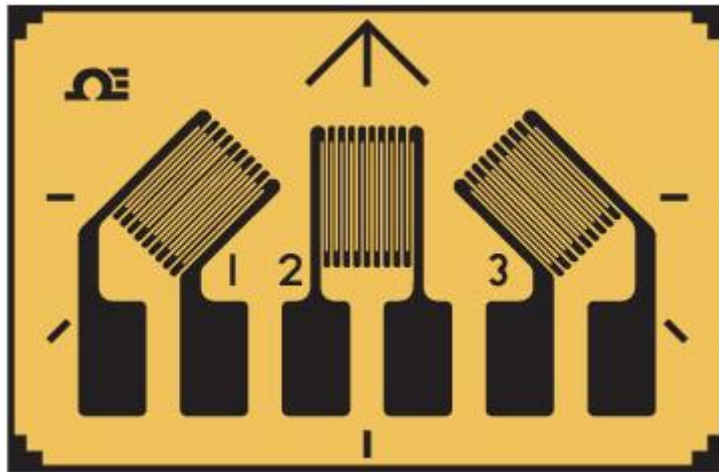


Figure 8: Strain gages in different directions (Gere, Goodno 2013)

5.2.1 Design

The crankshaft is considered a hollow rod/tube with an outer diameter of 24 mm and inner diameter of 19 mm made of aluminum 7020. A tube is very efficient in order to resist torsion, since the shear stresses are maximum at the outer surface and small close to the center. Hence, a tube is convenient for the application of a hand bike crankshaft, where material weight is preferred as low as possible.

The crankshaft is rotating during the propulsion cycle and a wireless system is essential to avoid conflicts with wires. Thus, a wireless system composed of an input sensor, wireless node, gateway and software was used (see figure 9) (LORD 2015). The input sensor is the strain gage (350 ohm V-rosette) mounted on the crankshaft. The sensor is connected with wires to a V-Link®-LXRS® Wireless 7 Channel analog input sensor node (LORD, corporation, Williston, USA), which is mounted on the left crank arm, thus the node follows the strain gages rotation. The node converts the analog signal from the strain gages to a digital signal and

transmits it wireless to the gateway (WSDA[®]-Base-101 Analog Output Base Station, LORD, Corporation, Williston, USA), which is connected to a computer running the node commander 2.17.0 software (LORD, corporation, Williston, USA).

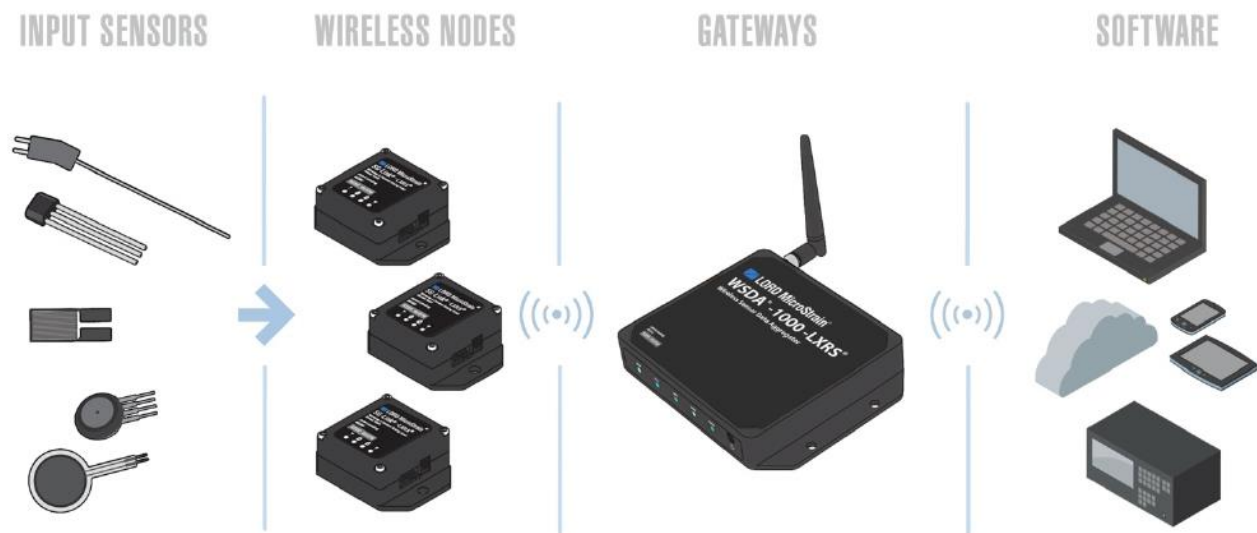


Figure 9: Illustration of sensor setup with node, gateway and software (LORD 2015).

As the principal normal stresses occur in an angle of $\pm 45^\circ$ with respect to the longitudinal axis of the crankshaft, the strain gage measurement angle must be orientated 45° as well (see figure 10).

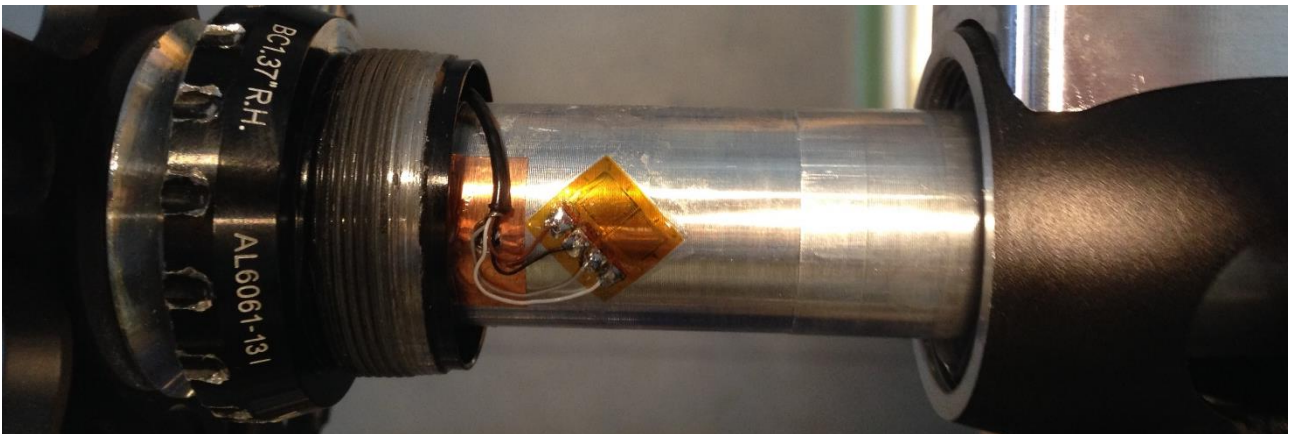


Figure 10: Strain gage orientation and location on crankshaft surface.

The strain gage setups follows the Wheatstone bridge circuit principal and forms a half-bridge setup as illustrated in figure 11.

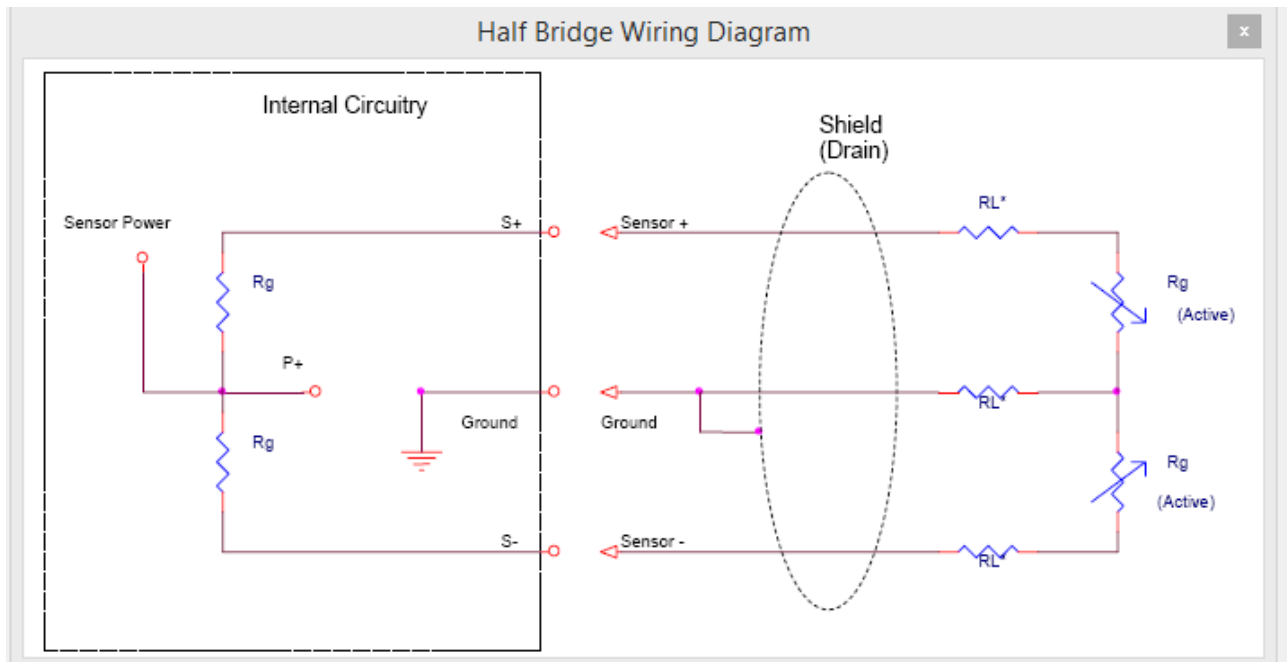


Figure 11: Illustration of half bridge wiring setup between input sensor and node (LORD 2015).

5.3 Crank position measurement

Position determination can be obtained using e.g. accelerometers, gyroscopes, cameras, GPS and encoders. The choice of sensor depends on what kind of position tracking is required. Accelerometers and gyroscopes are well suited for small position changes and GPS's are ideal for position tracking over larger areas. Encoders are often used in robots, engines and computers in order to track axel positions. They varies in sizes, accuracy, durability and amount of tracking information and simultaneously relatively small and cheap.

Requirements

- Detect crank position and angular velocity for each crank revolution
- Be low frictional in order to minimize braking effect

5.3.1 Design

The crank positioning measurement must provide information about the position and angular velocity of the crank arms during the propulsion cycle. Thus, it must be synchronized with the strain measurement from the strain gage on the crankshaft, in order to locate the force in relation to a specific crank position. The CAD of the crank positioning system was designed in SolidWorks 2015 (Dassault Systèmes SOLIDWORKS Corp., Massachusetts, USA) is presented in figure 12. A toothed wheel is clamped with a

custom made locking device onto the crankshaft. Another toothed wheel is connected to the crankshaft toothed wheel (exchange 1:1) and is mounted on a shaft entering a wheel encoder. Thus, one revolution of the crankshaft corresponds to one revolution for the wheel encoder. The technical drawings for the craftsmen are located in appendix.

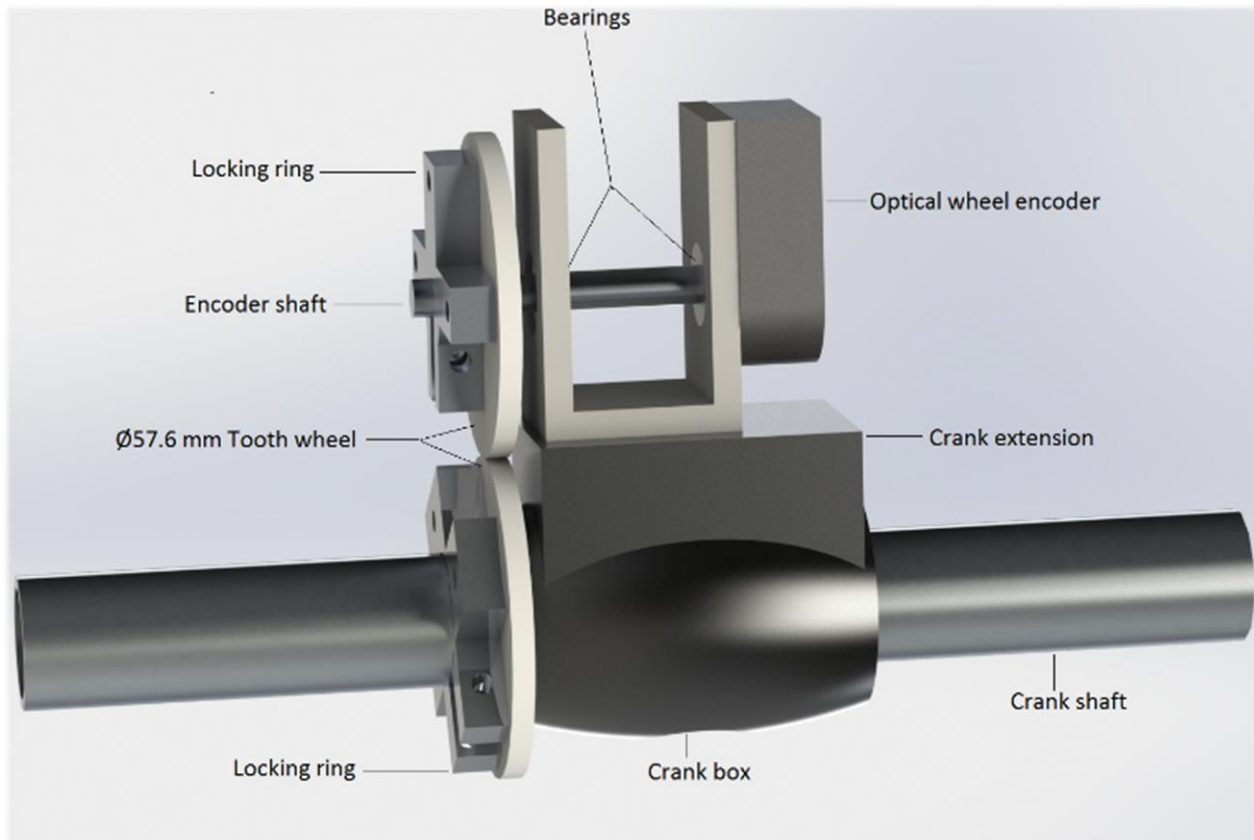


Figure 12: CAD model of the crank position measurement.

The encoder is specified as model HEDS-5540-A06 (Hewlett Hewlett Packard, California, USA), which is a three channel optical incremental encoder. The encoder implies a LED lensed course and a detector with output circuitry (see figure 13). The output of this setup is two square waves in quadrature with a 90° phase shift along with a third channel with a high true output index pulse generated once for each full rotation.

The encoder operates by the LED as light source. The light is then collimated through the lens into a parallel beam. Opposite of the lens is the detector section, which consists of multiple photodetectors along with the signal processing circuitry. Between the lens and the detector section a code wheel is placed to interrupt the light beam into different light patterns by spaces is the wheel (see figure 13). The detector section ends with three outputs, channel A, B and I.

Block Diagram

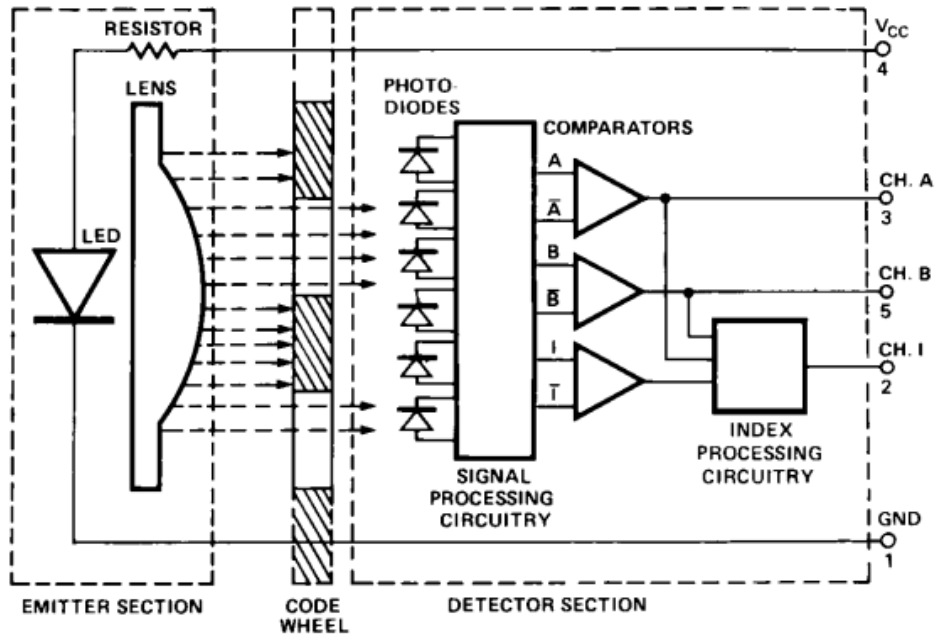


Figure 13: Block diagram for HEDS-5540-A06 (Hewlett).

The output waveform is 500 impulses per revolution for both channel A and B, for the I channel only one impulse per revolution. The A and B channels got a 90° phase shift, the reason therefore is to determine the direction of the rotation. If the A channel follows the B channel the code wheel spins counter-clockwise and visa versa (See figure 14). The encoder is mounted on top of the crank box (see figure 12).

Output Waveforms

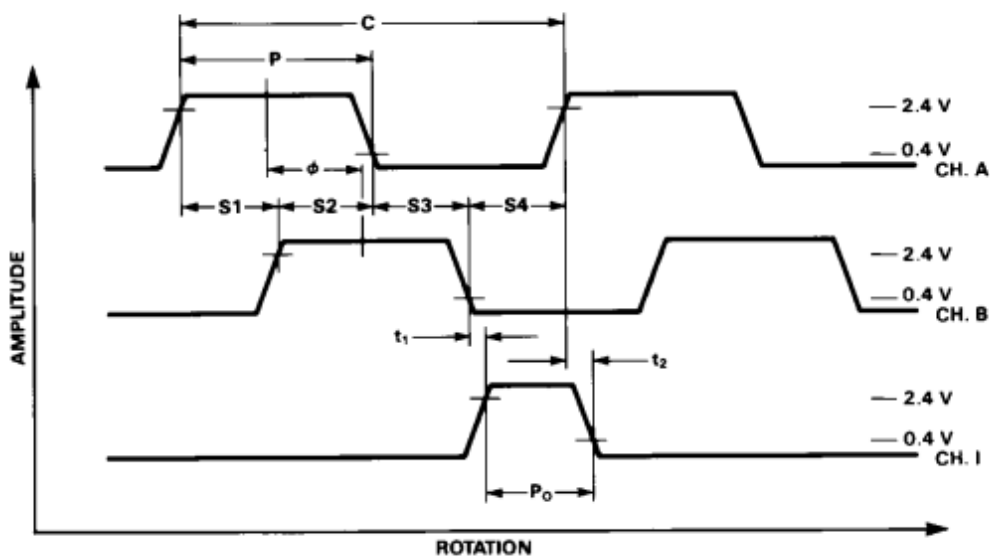


Figure 14: Output waveform for HEDS-5540-A06 (C) one cycle, (P) pulse width, (ϕ) phase. (Hewlett)

6 System implementation

In this chapter, the implementation of the hardware measurements and signals is presented. This implies the implementation of the kinematic propulsion data, kinetic of the propulsion data, in the musculoskeletal model in AnyBody.

6.1 Parameter identification –motion capture to musculoskeletal model

When a traditionally marker based motion capture system is used to drive the kinematics for a musculoskeletal model in AnyBody, the markers forms the basis for body segment scaling and determination of the human motion (Andersen et al. 2010). However, since there are no markers when using the Microsoft Kinect camera as motion capture, a different approach is considered in order to scale segments and drive the motion. Therefore, virtually markers are added to the stick figure, given from iPi Motion Capture Studio as illustrated in figure 15. This approach refers Andersen's and colleges work (Andersen 2013). The stick figure from iPi Motion Capture Studio is translated into a marker setup, which is able to drive the AMS musculoskeletal model.

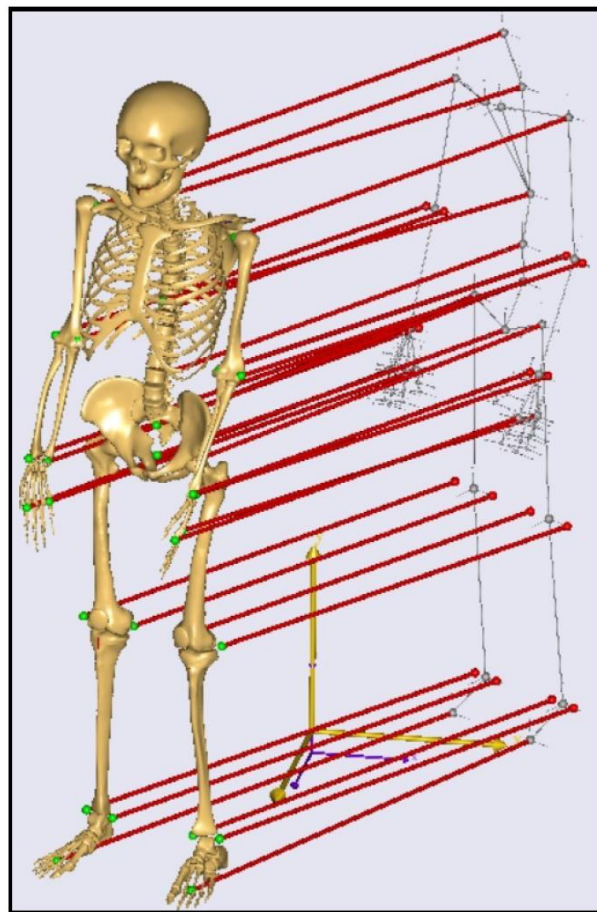


Figure 15: Scaling of musculoskeletal model corresponding to stick figure

Data synchronizing

This chapter describes the method for synchronizing the analog data from the strain gage (kinetics) and the encoder (position).

The voltage difference given from the strain gage when the crank shaft is subjected to torsion is digitized and transmitted wireless from the V-Link®-LXRS® Wireless 7 Channel analog input sensor node to the WSDA®-Base-101 Analog Output Base Station. The Base Station converts the digital signal to an analog signal and conveys it to an output pin panel. The pin panel is connected to a NI USB-6008/6009DAQ USB Device (National Instruments, Texas, USA), which digitizes the signal once again. The USB device samples with 16000 HZ for each channel.

The encoder mounted on the crank box is also connected to the USB device, where the analog impulses from the encoder is digitized.

The USB device setup with strain gage and encoder is illustrated in figure 16.

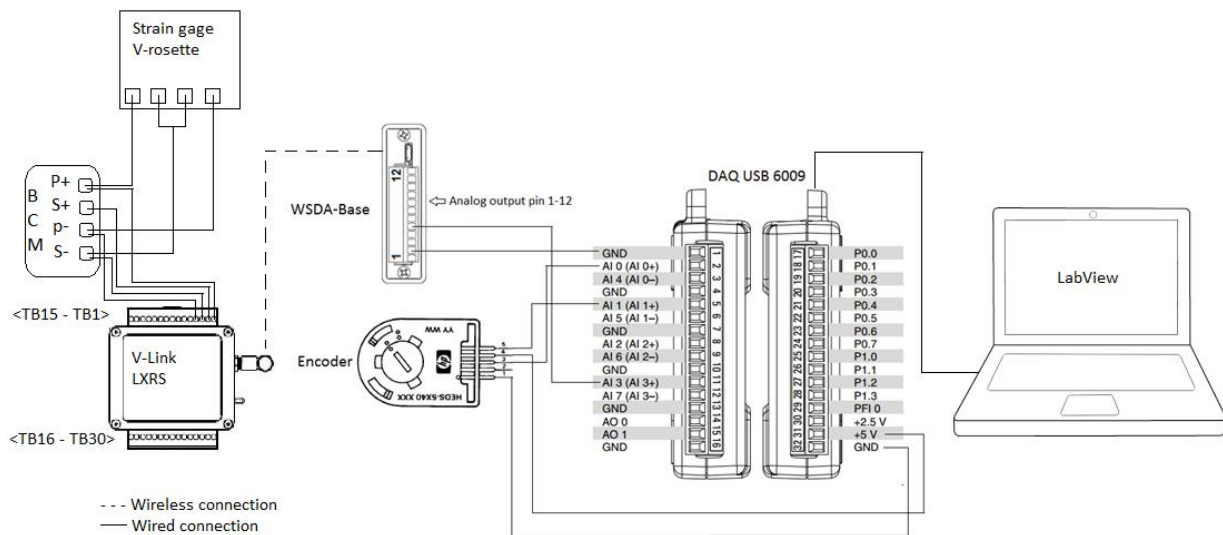


Figure 16: Data synchronizing setup.

When the signals from the encoder and the strain gage is digitized in the USB device the signals are sampled simultaneously, thus the position/speed and force data are synchronized. Figure 17 illustrates a GUI (guided user interface) setup in LabVIEW 2015 sp 1 (National Instruments, Texas, USA).

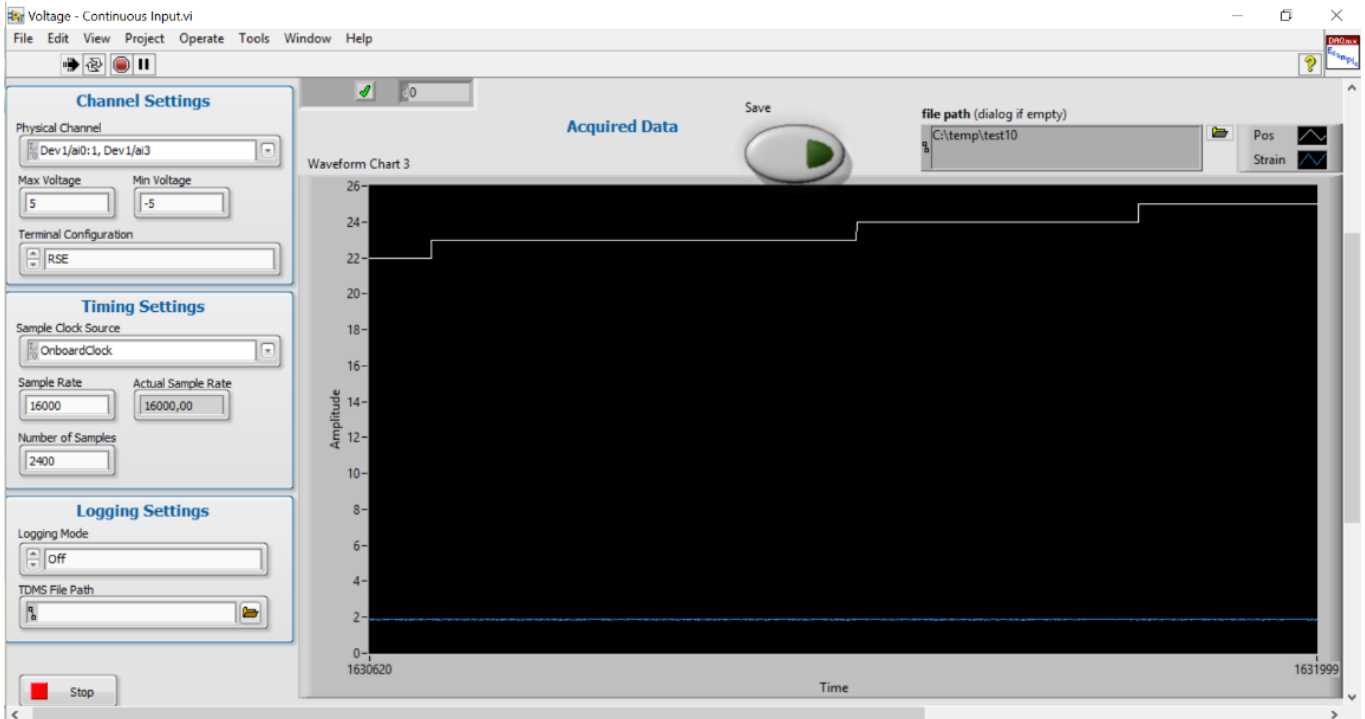


Figure 17: Labview GUI for position data and voltage data. The Blue line represents the voltage output from the strain gage and the white line represents crank position (500 impulses per revolution) with respect to time (second).

6.2 Calibration procedure

In order to determine the crank moment from the voltage output given from the strain gage, a calibration procedure was performed. Thus, a specific voltage output corresponded to a specific applied crank moment.

The crank was locked vertically in a vice as close to the crank box as possible. The pedal arms were placed horizontal at 90° with respect to vertical and crank tooth wheel fixed in this position. A string was fastened on the right pedal arm and loaded with 1,2,3,4 and 5 kilograms respectively. For every load, the voltage output from the strain gage changed and was sampled for five seconds. The average of the five second samples represented a measuring point for each load condition. The setup is illustrated in figure 18. The procedure was repeated three times with three different gains $\pm 1\text{mV}$ (gain 1214), $\pm 2.5\text{mV}$ (569) and $\pm 5\text{mV}$ (gain 291)). The calibration wizard in node commander was performed for all gains prior to applying loads (LORD 2015).

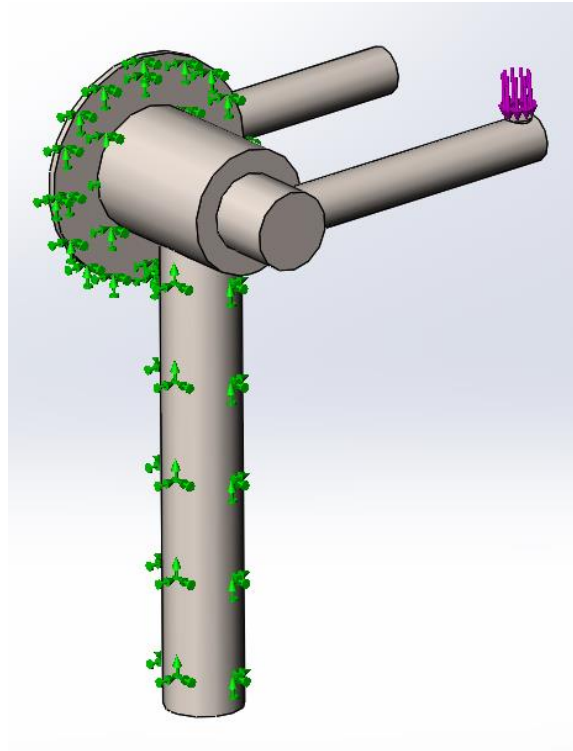


Figure 18: Calibration illustration (green arrows illustrates the fixed surfaces and the purple arrows represents applied force).



7 References

- Abel, T., Vega, S., Bleicher, I. & Platen, P. 2003, "Handbiking: Physiological Responses to Synchronous and Asynchronous Crank Montage", *European Journal of Sport Science*, vol. 3, no. 4, pp. 1-9.
- Andersen, M.S., Damsgaard, M., Macwilliams, B. & Rasmussen, J. 2010, "A computationally efficient optimisation-based method for parameter identification of kinematically determinate and over-determinate biomechanical systems", *Computer methods in biomechanics and biomedical engineering*, vol. 13, no. 2, pp. 171-183.
- Andersen, M.S. 2013, "Full-body musculoskeletal modeling using dual microsoft kinect sensors and the anybody modeling system", , pp. 23-24.
- Arnet, U. 2012a, "Development and validity of an instrumented handbike: initial results of propulsion kinetics", .
- Arnet, U. 2012b, *Handcycling: a biophysical analysis Chapter 1*, Amsterdam: Vrije Universiteit.
- Benoit, D.L., Ramsey, D.K., Lamontagne, M., Xu, L., Wretenberg, P. & Renström, P. 2006, "Effect of skin movement artifact on knee kinematics during gait and cutting motions measured in vivo", *Gait & posture*, vol. 24, no. 2, pp. 152-164.
- Bonnechère, B., Jansen, B., Salvia, P., Bouzahouene, H., Omelina, L., Moiseev, F., Sholukha, V., Cornelis, J., Rooze, M. & Van, S.J. 2014, "Validity and reliability of the Kinect within functional assessment activities: Comparison with standard stereophotogrammetry", *Gait & posture*, vol. 39, no. 1, pp. 593-598.
- Dallmeijer, A., J., Ottjes, L.,H.V., De Waardt, E, H.,V. & Van Der Woude, L, H.,V. 2004, "A Physiological Comparison of Synchronous and Asynchronous Hand Cycling", *International Journal of Sports Medicine*, vol. 25, no. 8, pp. 622-626.
- Faupin, A. & Gorce, P. 2008, "The effects of crank adjustments on handbike propulsion: A kinematic model approach", *International Journal of Industrial Ergonomics*, vol. 38, no. 7, pp. 577-583.
- Gere, M., James. & Goodno, J.B. 2013, "Chapter 7 - plane strain" in *Mechanics of Materials*, 8th edn, Gengage Learning, , pp. 661.
- Hettinga, F.J., Valent, L., Groen, W., Drongelen, v.S., Groot, d.S. & Woude. van der L.H.V 2010, "Hand-Cycling: An Active Form of Wheeled Mobility, Recreation, and Sports", *Phys Med Rehabil Clin*, vol. 21, pp. 127.
- Hewlett, P. *Quick Assembly Two and Three Channel Optical Encoders HEDS-5540-A06* .
- Khoshelham, K. 2012, "ACCURACY ANALYSIS OF KINECT DEPTH DATA", *The International Archives of the Photogrammetry, Remote Sensing and Spatial Information Sciences*, vol. XXXVIII-5/W12, pp. 133-138.
- Litzenberger, S., Mally, F., & Sabo, A. 2015, "**Influence of Different Seating and Crank Positions on Muscular Activity in Elite Handcycling - A Case Study**", *Procedia Engineering*, vol. 112, pp. 355.
- LORD, C. 2015, , *V-Link-LXRS Wireless Sensor Node User Manual*. Available: [http://files.microstrain.com/V-Link_User_Manual_\(8500-0006\).pdf](http://files.microstrain.com/V-Link_User_Manual_(8500-0006).pdf) [2016, .



- Neuman, M.R. 2000, "Physical Measurements." The Biomedical Engineering Handbook", vol. Second Edition, pp. Chapter 47.
- Rasmussen, J., Damsgaard, M. & Voigt, M. 2001, "Muscle recruitment by the min/ max criterion — a comparative numerical study", *Journal of Biomechanics*, vol. 34, no. 3, pp. 409-415.
- Riemer, R. & Hsiao-Weckler, E. 2008, "Improving joint torque calculations: Optimization- based inverse dynamics to reduce the effect of motion errors", *Journal of Biomechanics*, vol. 41, no. 7, pp. 1503-1509.
- Skals, S.L. 2015, *Prediction of ground reaction forces and moments during sports-related movements*.
- Vaughan, L.C., Davis, L.B. & Coonor, C.O.J., 1999, *Dynamics of Human Gait*, 2nd edition edn, Kiboho, South Africa.
- Zhou, H. & Hu, H. 2008, "Human motion tracking for rehabilitation—A survey", *Biomedical Signal Processing and Control*, vol. 3, no. 1, pp. 1-18.
- Zipfel, E., Olson, J., Puhlman, J. & Cooper, R.A. 2009, "Design of a custom racing hand- cycle: Review and analysis", *Disability & Rehabilitation: Assistive Technology*, 2009, vol. 4; Vol.4, no. 2; 2, pp. 119; 119-128; 128.